

Geodesic Difference-in-Differences

Yidong Zhou^{1,*}, Daisuke Kurisu^{2,*}, Taisuke Otsu³, and Hans-Georg Müller¹

¹Department of Statistics, University of California, Davis

²Center for Spatial Information Science, The University of Tokyo

³Department of Economics, London School of Economics

January 30, 2025

Abstract

Difference-in-differences (DID) is a widely used quasi-experimental design for causal inference, traditionally applied to scalar or Euclidean outcomes, while extensions to outcomes residing in non-Euclidean spaces remain limited. Existing methods for such outcomes have primarily focused on univariate distributions, leveraging linear operations in the space of quantile functions, but these approaches cannot be directly extended to outcomes in general metric spaces. In this paper, we propose geodesic DID, a novel DID framework for outcomes in geodesic metric spaces, such as distributions, networks, and manifold-valued data. To address the absence of algebraic operations in these spaces, we use geodesics as proxies for differences and introduce the geodesic average treatment effect on the treated (ATT) as the causal estimand. We establish the identification of the geodesic ATT and derive the convergence rate of its sample versions, employing tools from metric geometry and empirical process theory. This framework is further extended to the case of staggered DID settings, allowing for multiple time periods and varying treatment timings. To illustrate the practical utility of geodesic DID, we analyze health impacts of the Soviet Union's collapse using age-at-death distributions and assess effects of U.S. electricity market liberalization on electricity generation compositions.

Keywords: Difference-in-differences, Fréchet mean, geodesic space, network, optimal transport

*The first two authors contributed equally to this work.

[†]D.K. was supported in part by JSPS KAKENHI Grant Number 23K12456. H.G.M. was partially supported by NSF grant DMS-2310450.

1 Introduction

Difference-in-differences (DID) is widely used to study the causal effect of an intervention, such as a policy change, a new social or healthcare program, or an unexpected event, by exploiting observational panel data. Under the assumption that average outcomes of control and treated groups in the absence of an intervention obey parallel trends over time, DID identifies the average treatment effect on the treated (ATT) by comparing average outcomes of those groups for pre- and post-intervention periods, and estimation and inference on the DID model are typically conducted via two-way fixed effects regression. DID is applied in various fields of data science, such as economics ([Angrist and Pischke, 2009](#)), epidemiology and public health ([Wing et al., 2018](#)), management science ([Antonakis et al., 2010](#)), marketing ([Varian, 2016](#)), and political science ([Keele, 2015](#)).

Since its beginnings (e.g., [Card and Krueger, 1994](#)), the methodology of DID has been extended in various directions. For example, [Athey and Imbens \(2006\)](#) proposed the changes-in-changes approach to allow heterogeneous treatment effects and infer the counterfactual distribution for the treated group; see [Torous et al. \(2024\)](#) for an extension to multivariate outcomes and [Biewen et al. \(2022\)](#) for an alternative approach using distribution regression. Other developments in the DID framework involve its integration with instrumental variables ([Ye et al., 2023](#)) and adaptations to factorial designs ([Xu et al., 2024](#)). Researchers have also extensively examined the fundamental parallel trends assumption ([Sofer et al., 2016](#); [Roth and Sant'Anna, 2023](#)), which underpins the validity of DID estimates. In the context of staggered treatment adoption, [Callaway and Sant'Anna \(2021\)](#) provided key insights into identification and estimation, with additional contributions from [Ding and Li \(2019\)](#) and [Ben-Michael et al. \(2022\)](#), and a comprehensive overview of the topic by [Roth et al. \(2023\)](#).

In modern data science, one increasingly encounters complex-structured data, such as networks (Zhou and Müller, 2022), distributions (Petersen et al., 2022), compositional data (Scealy and Welsh, 2011) or trees (Nye et al., 2017). Such data are inherently non-Euclidean and can be viewed as elements of a metric space. Addressing causal inference for metric space-valued data is a very recent development and includes doubly robust estimators for distributional outcomes (Lin et al., 2023), for outcomes residing in general geodesic metric spaces (Kurisu et al., 2024) and also the synthetic control method for distributional outcomes (Gunsilius, 2023). Nevertheless, almost all existing DID methodologies have remained focused on scalar or Euclidean outcomes, with the exception of Opoku-Agyemang (2023), where causal effects on distributional outcomes are studied within the DID framework. This approach leverages restricted linear operations in the space of quantile functions but is limited to univariate distributions and cannot be extended to general metric spaces.

In this paper, we introduce geodesic DID, a novel framework for DID analysis of outcomes residing in non-Euclidean spaces, specifically geodesic metric spaces. To address the absence of algebraic operations like addition and scalar multiplication in these spaces, we utilize geodesics as proxies for differences and define the geodesic ATT as the causal estimand. We establish the identification of the geodesic ATT and derive the convergence rate of empirical estimators, using tools from metric geometry and working within the space of geodesics. Additionally, we extend the framework to the staggered DID settings, incorporating multiple time periods and variation in treatment timing.

The paper is organized as follows. In Section 2, we present a brief review of geodesic spaces and the geodesics in such spaces. The geodesic DID framework is introduced in Section 3, with the asymptotic convergence rate established in Section 4. Simulations for distributional and network outcomes are presented in Section 5. Section 6 demonstrates

the practical relevance of geodesic DID through two applications where we investigate the health consequences of the Soviet Union's collapse as reflected in age-at-death distributions and examine the impact of U.S. electricity market liberalization on electricity generation compositions. A theoretical extension to staggered DID is discussed in Section 7, followed by concluding remarks in Section 8. Proofs of theoretical results are deferred to the Supplementary Material.

2 Preliminaries on Geodesic Calculus

Let (\mathcal{M}, d) be a bounded and separable metric space. A *curve* in \mathcal{M} is a continuous map $\gamma : [a, b] \rightarrow \mathcal{M}$ with length

$$L(\gamma) = \sup \sum_{k=0}^{K-1} d\{\gamma(t_k), \gamma(t_{k+1})\},$$

where the supremum is taken over all $K \geq 1$ and partitions $a = t_0 \leq t_1 \leq \dots \leq t_K = b$ and the curve is rectifiable if $L(\gamma) < \infty$. Two curves γ_1 and γ_2 are said to be equivalent if $\gamma_1 \circ \phi_1 = \gamma_2 \circ \phi_2$ for non-decreasing and continuous functions ϕ_1 and ϕ_2 . In this case, γ_1 is said to be a reparametrisation of γ_2 and we check that $L(\gamma_1) = L(\gamma_2)$. A curve $\gamma : [a, b] \rightarrow \mathcal{M}$ is said to have constant speed if for all $a \leq s \leq t \leq b$,

$$L(\gamma_{[s,t]}) = \frac{t-s}{b-a} L(\gamma),$$

where $\gamma_{[s,t]}$ denotes the restriction of γ to $[s, t]$.

Given $\alpha, \beta \in \mathcal{M}$, a curve $\gamma : [a, b] \rightarrow \mathcal{M}$ is said to connect α to β if $\gamma(a) = \alpha$ and $\gamma(b) = \beta$. By construction of the length function L , $d(\alpha, \beta) \leq L(\gamma)$ for any curve γ connecting α to β . The space \mathcal{M} is called a *length space* if, for all $\alpha, \beta \in \mathcal{M}$,

$$d(\alpha, \beta) = \inf_{\gamma} L(\gamma), \tag{1}$$

where the infimum is taken over all curves γ connecting α to β . A length space is said to be a *geodesic space* if, for all $\alpha, \beta \in \mathcal{M}$, the infimum on the right-hand side of (1) is attained.

In a geodesic space, we call *geodesic* between α and β any constant speed reparametrization $\gamma : [0, 1] \rightarrow \mathcal{M}$ of a curve attaining the infimum in (1). The geodesic connecting α and β is denoted as $\gamma_{\alpha, \beta}$. If there exists only one such geodesic for all $\alpha, \beta \in \mathcal{M}$, the space \mathcal{M} is referred to as a *unique geodesic space* (Bridson and Haefliger, 1999).

For points $\alpha, \beta, \zeta \in \mathcal{M}$, we define the following operations on geodesics. The concatenation of two geodesics $\gamma_{\alpha, \zeta}$ and $\gamma_{\zeta, \beta}$ is given by $\gamma_{\alpha, \zeta} \oplus \gamma_{\zeta, \beta} := \gamma_{\alpha, \beta}$, while the reversal of a geodesic $\gamma_{\alpha, \beta}$ is defined as $\ominus \gamma_{\alpha, \beta} := \gamma_{\beta, \alpha}$. The difference between two geodesics with a common start point is defined as $\ominus \gamma_{\zeta, \alpha} \oplus \gamma_{\zeta, \beta} := \gamma_{\alpha, \beta}$. These operations naturally extend the concepts of addition, reversal, and subtraction from Euclidean space to the context of geodesic spaces; these notions also underpin previous work on the doubly robust estimation of average treatment effect in geodesic spaces (Kurisu et al., 2024).

Next, we present examples of unique geodesic spaces encountered in real-world applications. We use these example spaces to demonstrate the practical performance of the proposed approach in simulations and data analyses. In Section S.2 of the Supplementary Material, we demonstrate that these examples satisfy the pertinent assumptions in Section 4.

Example 1 (Wasserstein space). *The Wasserstein space $(\mathcal{W}, d_{\mathcal{W}})$ consists of univariate distributions on \mathbb{R} with finite second moments, equipped with the Wasserstein distance $d_{\mathcal{W}}$. This space is both complete and separable (Panaretos and Zemel, 2020). The Wasserstein distance between two distributions μ_1 and μ_2 is*

$$d_{\mathcal{W}}^2(\mu_1, \mu_2) = \int_0^1 \{F_{\mu_1}^{-1}(p) - F_{\mu_2}^{-1}(p)\}^2 dp,$$

where $F_{\mu_1}^{-1}(\cdot)$, $F_{\mu_2}^{-1}(\cdot)$ are the quantile functions of μ_1 and μ_2 , respectively. This space

provides a natural framework for studying distributions as geometric objects, with geodesics defined explicitly through optimal transport maps.

Example 2 (Space of compositional data). *Compositional data, which are represented as proportions summing to 1, reside in the simplex*

$$\Delta^{d-1} = \{\mathbf{y} \in \mathbb{R}^d : y_j \geq 0, j = 1, \dots, d, \text{ and } \sum_{j=1}^d y_j = 1\}.$$

Through the component-wise square root transformation $\sqrt{\mathbf{y}} = (\sqrt{y_1}, \dots, \sqrt{y_d})'$, the simplex can be mapped to the first orthant of the unit sphere (Scealy and Welsh, 2011, 2014):

$$\mathcal{S}_+^{d-1} = \{\mathbf{z} \in \mathcal{S}^{d-1} : z_j \geq 0, j = 1, \dots, d\}.$$

Equipping \mathcal{S}_+^{d-1} with the geodesic (Riemannian) metric on the sphere,

$$d_g(\mathbf{z}_1, \mathbf{z}_2) = \arccos(\mathbf{z}_1' \mathbf{z}_2), \quad \text{for } \mathbf{z}_1, \mathbf{z}_2 \in \mathcal{S}_+^{d-1},$$

induces a unique geodesic structure.

Example 3 (Space of networks/covariance matrices). *Consider the space of simple, undirected, weighted networks with a fixed number of nodes m and bounded edge weights. Each such network is uniquely represented by its graph Laplacian. The space of graph Laplacians equipped with the Frobenius distance d_F can thus be used to characterize the space of networks (Zhou and Müller, 2022). Similarly, the space of m -dimensional covariance matrices with bounded diagonal entries forms a bounded, convex subset of \mathbb{R}^{m^2} when endowed with d_F (Dryden et al., 2009).*

Write $T_{\#}\mu$ for the pushforward measure of μ by the transport T . In the Wasserstein space introduced in Example 1, the geodesic between two distributions $\alpha, \beta \in \mathcal{W}$ is given by McCann's interpolant (McCann, 1997),

$$\gamma_{\alpha, \beta}(t) = (\text{id} + t(F_{\beta}^{-1} \circ F_{\alpha} - \text{id}))_{\#}\alpha,$$

where id denotes the identity map, and F_α and F_β^{-1} are the cumulative distribution function of α and the quantile function of β , respectively.

For compositional data the geodesic connecting two points $\alpha, \beta \in \mathcal{S}_+^{d-1}$ is given by

$$\gamma_{\alpha,\beta}(t) = \cos(\theta t)\alpha + \sin(\theta t)\frac{\beta - (\alpha'\beta)\alpha}{\|\beta - (\alpha'\beta)\alpha\|},$$

where $\theta = \arccos(\alpha'\beta)$ is the angle between α and β . Finally, for both networks and covariance matrices, the geodesic connecting two matrices α, β is

$$\gamma_{\alpha,\beta}(t) = \alpha + (\beta - \alpha)t, \quad t \in [0, 1].$$

3 Geodesic Difference-in-Differences

Consider the “canonical” difference-in-differences (DID) model with Euclidean outcomes in which there are two time periods, $t = 0, 1$. Units $i = 1, \dots, n$ are either given a treatment or untreated. Let D_i be a binary variable with $D_i = 1$ if unit i is treated and $D_i = 0$ otherwise. For unit i at time t , we observe a treatment indicator variable $D_{i,t}$ where $D_{i,t} = 1$ if unit i is treated and $D_{i,t} = 0$ otherwise, along with a Euclidean outcome $Y_{i,t} = D_{i,t}Y_{i,t}(1) + (1 - D_{i,t})Y_{i,t}(0)$ where $Y_{i,t}(0), Y_{i,t}(1)$ are potential outcomes for $D_{i,t} = 0$ and 1, respectively. This potential outcomes framework implicitly encodes the *stable unit treatment value assumption (SUTVA)* that for all i the outcome for unit i does not depend on the treatment status of units $j \neq i$, which rules out spillover and general equilibrium effects (Roth et al., 2023). We assume that units from the treated population ($D_i = 1$) receive a treatment of interest between period $t = 0$ and $t = 1$, whereas units from the untreated (a.k.a. comparison or control) population ($D_i = 0$) remain untreated in both

time periods, i.e.,

$$D_i = 0 \Rightarrow D_{i,0} = 0, D_{i,1} = 0, \quad (2)$$

$$D_i = 1 \Rightarrow D_{i,0} = 0, D_{i,1} = 1. \quad (3)$$

The causal estimand of interest is the *average treatment effect on the treated* (ATT), $\tau = E\{Y_{i,1}(1) - Y_{i,1}(0)|D_i = 1\}$. Then under the parallel trends assumption that

$$E\{Y_{i,1}(0) - Y_{i,0}(0)|D_i = 1\} = E\{Y_{i,1}(0) - Y_{i,0}(0)|D_i = 0\},$$

the ATT is identified by the canonical DID estimand

$$\tau = E\{Y_{i,1} - Y_{i,0}|D_i = 1\} - E\{Y_{i,1} - Y_{i,0}|D_i = 0\}. \quad (4)$$

Now consider the outcome $Y_{i,t}$ to be a random object residing in a unique geodesic space (\mathcal{M}, d) . In what follows, we assume the STUVA at each time point, i.e.,

$$Y_{i,t} = \begin{cases} Y_{i,t}(0) & \text{if } D_{i,t} = 0, \\ Y_{i,t}(1) & \text{if } D_{i,t} = 1, \end{cases}$$

additional conditions regarding the timing of receiving the treatment (Conditions (2) and (3)) and that $\{(Y_{i,0}, Y_{i,1}, D_i)\}_{i=1}^n$ is an i.i.d. sample drawn from a joint distribution P ; a generic random variable distributed according to P is $(Y_0, Y_1, D) \in \mathcal{M} \times \mathcal{M} \times \{0, 1\}$.

For a random object $Y \in \mathcal{M}$, the Fréchet mean of Y , extending the usual notion of mean, is

$$E_{\oplus}(Y) = \arg \min_{\omega \in \mathcal{M}} E\{d^2(Y, \omega)\},$$

where the existence and uniqueness of the minimizer is guaranteed for Hadamard spaces (Sturm, 2003) and the example spaces described in Examples 1–3. The conditional Fréchet mean of Y given $X \in \mathbb{R}^p$ (Petersen and Müller, 2019) is analogously defined as

$$E_{\oplus}(Y|X) = \arg \min_{\omega \in \mathcal{M}} E\{d^2(Y, \omega)|X\}.$$

To obtain the DID estimand for outcomes in \mathcal{M} , it is necessary to define a notion of subtraction in the unique geodesic space \mathcal{M} . We borrow from Kurisu et al. (2024) an approach to represent differences as geodesics, quantifying the difference between two points $\alpha, \beta \in \mathcal{M}$ as the geodesic $\gamma_{\alpha, \beta}$. In the canonical DID estimand (4), a second difference is computed between two differences for the treated and control groups. Extending this concept to \mathcal{M} requires quantifying differences between geodesics, which can be achieved with geodesic transport maps under the ubiquity assumption (Zhu and Müller, 2023).

Assumption 3.1. *Let (\mathcal{M}, d) be a unique geodesic space. For any two points $\alpha, \beta \in \mathcal{M}$, there exists a geodesic transport map $\Gamma_{\alpha, \beta} : \mathcal{M} \rightarrow \mathcal{M}$ with the following property: for any $\omega \in \mathcal{M}$, there exists a unique point $\zeta \in \mathcal{M}$ such that $\Gamma_{\alpha, \beta}(\omega) = \zeta$.*

This assumption ensures that any geodesic $\gamma_{\alpha, \beta}$ can be naturally extended from any point $\omega \in \mathcal{M}$ to produce a new geodesic $\gamma_{\omega, \zeta}$, which terminates at a unique point $\zeta \in \mathcal{M}$. The map $\Gamma_{\alpha, \beta}$ is naturally defined in the Euclidean setting \mathbb{R}^p , where $\Gamma_{\alpha, \beta}(\omega) = \omega + (\beta - \alpha)$ for any $\alpha, \beta, \omega \in \mathbb{R}^p$. This construction extends to any vector space, where geodesics represent the vectors connecting two points and also to Riemannian manifolds using parallel transport (Yuan et al., 2012; Lin and Yao, 2019; Chen et al., 2023a). Specifications of geodesic transport maps for Examples 1–3 are provided in Section S.1 of the Supplementary Material.

We now extend the notion of subtraction to geodesics with different starting points by aligning the subtrahend with the minuend using the geodesic transport map.

Definition 3.1. *For any points $\alpha, \beta, \omega, \zeta \in \mathcal{M}$ with $\alpha \neq \omega$, the difference between two geodesics is defined as*

$$\ominus \gamma_{\alpha, \beta} \oplus \gamma_{\omega, \zeta} := \ominus \gamma_{\omega, \zeta'} \oplus \gamma_{\omega, \zeta} = \gamma_{\zeta', \zeta},$$

where $\zeta' = \Gamma_{\alpha, \beta}(\omega)$.

The above operation is straightforward in the vector space \mathbb{R}^p where $\zeta' = \omega + \beta - \alpha$ and we verify that $\zeta - \zeta' = -(\beta - \alpha) + (\zeta - \omega)$.

Let $\nu_{d,t}(0) = E_{\oplus}(Y_{i,t}(0)|D_i = d)$ and $\nu_{d,t}(1) = E_{\oplus}(Y_{i,t}(1)|D_i = d)$ for $d, t \in \{0, 1\}$. We introduce the following notions of causal effects in unique geodesic spaces.

Definition 3.2 (Geodesic ATT). *The geodesic average treatment effect on the treated (GATT) τ is defined as the geodesic connecting $\nu_{1,1}(0)$ and $\nu_{1,1}(1)$, i.e., $\tau = \gamma_{\nu_{1,1}(0), \nu_{1,1}(1)}$.*

The GATT is a geodesic, with its direction and length capturing the direction and magnitude of the causal effect when outcomes are random objects in unique geodesic spaces.

Assumption 3.2. $\Gamma_{\nu_{0,0}(0), \nu_{0,1}(0)}(\nu_{1,0}(0)) = \nu_{1,1}(0)$.

Assumption 3.2 is a direct generalization of the parallel trends assumption to the unique geodesic space. It asserts that in the absence of treatment, the geodesic connecting the control group's outcomes in the pre- and post-treatment periods, when extended from the treated group's pre-treatment outcome, should end at the treated group's post-treatment outcome. This ensures that, without treatment, the trajectory of outcomes for the treated group aligns with the control group's geodesic trend; see Figure 1 for an illustration. In the case of Euclidean outcome, Assumption 3.2 reduces to $\nu_{1,0}(0) + \{\nu_{0,1}(0) - \nu_{0,0}(0)\} = \nu_{1,1}(0)$, which corresponds to the standard parallel trends assumption in the canonical DID framework.

Writing $\nu_{d,t} = E_{\oplus}(Y_{i,t}|D_i = d)$ for $d, t \in \{0, 1\}$, GATT can be identified as follows.

Theorem 3.1. *Suppose that Assumptions 3.1 and 3.2 hold. Then we have*

$$\tau = \ominus \gamma_{\nu_{0,0}, \nu_{0,1}} \oplus \gamma_{\nu_{1,0}, \nu_{1,1}} = \gamma'_{\nu'_{1,1}, \nu_{1,1}}, \quad (5)$$

where $\ominus \gamma_{\nu_{0,0}, \nu_{0,1}} \oplus \gamma_{\nu_{1,0}, \nu_{1,1}}$ is the geodesic DID estimand and $\nu'_{1,1} = \Gamma_{\nu_{0,0}, \nu_{0,1}}(\nu_{1,0})$.

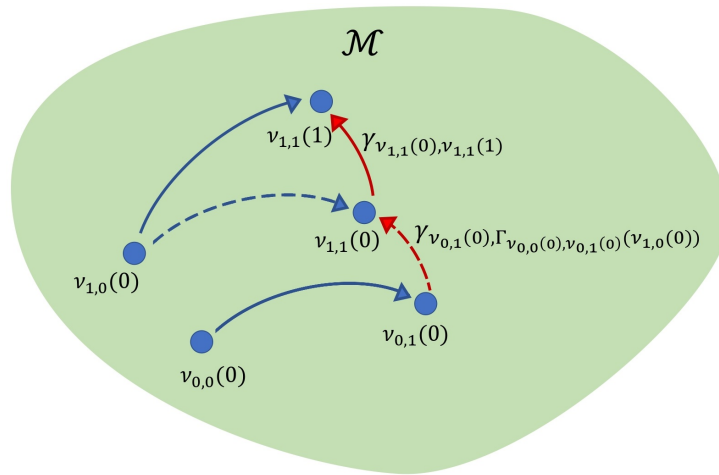


Figure 1: Illustration of geodesic DID. The blue solid circles symbolize objects in the unique geodesic space \mathcal{M} . The arrows emanating from the circles represent the geodesic paths connecting them. The red arrows represent the geodesic transport from $\nu_{0,1}(0)$ to $\nu_{1,1}(0)$ and the proposed GATT.

Consider the special case of a Euclidean space, $(\mathcal{M}, d) = (\mathbb{R}, \|\cdot\|)$, where $\|\cdot\|$ is the standard Euclidean metric. Note that for any $\alpha, \beta, \omega \in \mathcal{M}$, the geodesic is the line segment that connects α and β , i.e., $\gamma_{\alpha, \beta}(t) = \alpha + t(\beta - \alpha)$ and the geodesic transport map determined by α and β is given as $\Gamma_{\alpha, \beta}(\omega) = \omega + \beta - \alpha$. The start and end points of the geodesic DID estimand $\ominus \gamma_{\nu_{0,0}, \nu_{0,1}} \oplus \gamma_{\nu_{1,0}, \nu_{1,1}}$ are thus $\nu_{1,1}$ and $\nu_{1,0} + (\nu_{0,1} - \nu_{0,0})$, respectively. Then under the parallel trends assumption, for the length of the geodesic DID estimand, corresponding to the canonical DID estimand, one has

$$\begin{aligned} \nu_{1,1} - \{\nu_{1,0} + (\nu_{0,1} - \nu_{0,0})\} &= (\nu_{1,1} - \nu_{1,0}) - (\nu_{0,1} - \nu_{0,0}) \\ &= E\{Y_{i,1} - Y_{i,0} | D_i = 1\} - E\{Y_{i,1} - Y_{i,0} | D_i = 0\} = E\{Y_{i,1}(1) - Y_{i,1}(0) | D_i = 1\}. \end{aligned}$$

Therefore, Theorem 3.1 can be seen as an extension of the identification of ATT $\tau = E\{Y_{i,1}(1) - Y_{i,1}(0) | D_i = 1\}$ in the Euclidean setting to unique geodesic spaces.

4 Estimation and Theory

Given a sample $\{(Y_{i,0}, Y_{i,1}, D_i)\}_{i=1}^n$, the geodesic DID estimand of the GATT, namely $\tau = \gamma_{\nu'_{1,1}, \nu_{1,1}}$, is estimated by substituting the sample version for the Fréchet means

$$\hat{\tau} = \gamma_{\hat{\nu}'_{1,1}, \hat{\nu}_{1,1}}, \quad \hat{\nu}'_{1,1} = \Gamma_{\hat{\nu}_{0,0}, \hat{\nu}_{0,1}}(\hat{\nu}_{1,0}), \quad (6)$$

where for $t \in \{0, 1\}$,

$$\begin{aligned} \hat{\nu}_{0,t} &= \arg \min_{\omega \in \mathcal{M}} \frac{1}{n_0} \sum_{i=1}^n (1 - D_i) d^2(Y_{i,t}, \omega), \quad n_0 = \sum_{i=1}^n (1 - D_i), \\ \hat{\nu}_{1,t} &= \arg \min_{\omega \in \mathcal{M}} \frac{1}{n_1} \sum_{i=1}^n D_i d^2(Y_{i,t}, \omega), \quad n_1 = \sum_{i=1}^n D_i. \end{aligned}$$

Our goal is to establish the consistency of $\hat{\tau}$ in (6) and to derive its convergence rate. Since τ is a geodesic, a properly defined metric on the space of geodesics is required to evaluate the performance of $\hat{\tau}$. We begin by defining the space of geodesics.

Definition 4.1. *The space of geodesics on the unique geodesic space (\mathcal{M}, d) is*

$$\mathcal{G}(\mathcal{M}) = \{\gamma_{\alpha, \beta} : \alpha, \beta \in \mathcal{M}\}.$$

To compare geodesics, we define a binary relation \sim on $\mathcal{G}(\mathcal{M})$ through the geodesic transport map, where $\gamma_{\alpha_1, \beta_1} \sim \gamma_{\alpha_2, \beta_2}$ if and only if $\Gamma_{\alpha_1, \beta_1}(\omega) = \Gamma_{\alpha_2, \beta_2}(\omega)$ for all $\omega \in \mathcal{M}$.

Proposition 4.1. *The relation \sim is an equivalence relation on $\mathcal{G}(\mathcal{M})$.*

This equivalence relation, drawing on the ubiquity Assumption 3.1, partitions the space of geodesics $\mathcal{G}(\mathcal{M})$ into disjoint equivalence classes. The equivalence class of $\gamma_{\alpha, \beta} \in \mathcal{G}(\mathcal{M})$ is denoted by $[\gamma_{\alpha, \beta}]$. The set of all equivalence classes $\mathcal{G}(\mathcal{M}) / \sim := \{[\gamma_{\alpha, \beta}] : \gamma_{\alpha, \beta} \in \mathcal{G}(\mathcal{M})\}$ is the quotient space of $\mathcal{G}(\mathcal{M})$, for which we define a metric as follows. For any $[\gamma_{\alpha_1, \beta_1}], [\gamma_{\alpha_2, \beta_2}] \in \mathcal{G}(\mathcal{M}) / \sim$,

$$d_{\mathcal{G}}([\gamma_{\alpha_1, \beta_1}], [\gamma_{\alpha_2, \beta_2}]) = d_{\mathcal{G}, \omega_{\oplus}}([\gamma_{\alpha_1, \beta_1}], [\gamma_{\alpha_2, \beta_2}]) = d(\Gamma_{\alpha_1, \beta_1}(\omega_{\oplus}), \Gamma_{\alpha_2, \beta_2}(\omega_{\oplus})), \quad (7)$$

where $\omega_{\oplus} \in \mathcal{M}$ is a fixed reference point, chosen e.g., as the Fréchet mean of the outcome.

Proposition 4.2. $d_{\mathcal{G}}$ is a metric on the quotient space $\mathcal{G}(\mathcal{M})/\sim$.

$(\mathcal{G}(\mathcal{M})/\sim, d_{\mathcal{G}})$ is thus a metric space, and the estimation error of $\hat{\tau}$ can be quantified by $d_{\mathcal{G}}(\hat{\tau}, \tau)$, where the reference point is chosen as $\nu'_{1,1} = \Gamma_{\nu_{0,0}, \nu_{0,1}}(\nu_{1,0})$. We require the following regularity assumptions.

Assumption 4.1. *There exists a constant $C_1 > 0$ such that for any $\alpha, \beta, \omega, \zeta \in \mathcal{M}$, $d(\Gamma_{\alpha, \beta}(\omega), \Gamma_{\alpha, \beta}(\zeta)) \leq C_1 d(\omega, \zeta)$.*

Assumption 4.2. *There exists a constant $C_2 > 0$ such that for any $\alpha_1, \alpha_2, \beta_1, \beta_2, \omega \in \mathcal{M}$, $d(\Gamma_{\alpha_1, \beta_1}(\omega), \Gamma_{\alpha_2, \beta_2}(\omega)) \leq C_2 \{d(\alpha_1, \alpha_2) + d(\beta_1, \beta_2)\}$.*

Assumption 4.1 enforces Lipschitz continuity on the geodesic transport map. Assumption 4.2 ensures that, for any two geodesics, when both are moved to the same starting point, the distance between their new endpoints is bounded by the sum of the distances between their original starting points and endpoints. These two assumptions are trivially satisfied in Euclidean spaces with $C_1 = C_2 = 1$.

Assumption 4.3. *For $d, t \in \{0, 1\}$, the following conditions hold.*

(i) *The population Fréchet mean $\nu_{d,t}$ and its empirical counterpart $\hat{\nu}_{d,t}$ exist and are unique, the latter almost surely, and, for any $\varepsilon > 0$, $\inf_{d(\nu_{d,t}, \omega) > \varepsilon} E\{d^2(Y_t, \omega) | D\} > E\{d^2(Y_t, \nu_{d,t}) | D\}$.*

(ii) *Let $B_{\delta}(\nu_{d,t}) \subset \mathcal{M}$ be the ball of radius δ centered at $\nu_{d,t}$ and $N(\epsilon, B_{\delta}(\nu_{d,t}), d)$ be its covering number using balls of size ϵ . Then*

$$\int_0^1 \sqrt{1 + \log N(\delta\epsilon, B_{\delta}(\nu_{d,t}), d)} \, d\epsilon = O(1) \quad \text{as } \delta \rightarrow 0.$$

(iii) There exist $\eta > 0$, $C > 0$ and $\kappa > 1$ such that, whenever $d(\nu_{d,t}, \omega) < \eta$, we have

$$E\{d^2(Y_t, \omega)|D\} - E\{d^2(Y_t, \nu_{d,t})|D\} \geq Cd^\kappa(\nu_{d,t}, \omega).$$

Assumption 4.3 (i) is a standard requirement for establishing the consistency of M-estimators, such as the Fréchet mean; see [van der Vaart and Wellner \(2023\)](#), Chapter 3.2. This assumption ensures that the weak convergence of the empirical process to the population process entails the convergence of their respective minimizers. Additionally, the existence of the minimizer is guaranteed if the unique geodesic space \mathcal{M} is compact. The conditions on the covering number in Assumption 4.3 (ii) and the curvature in Assumption 4.3 (iii) arise from empirical process theory and regulate the behavior of the difference between the empirical and population processes near the minimum. We verify the validity of Assumptions 4.1–4.3 for the examples presented in Examples 1–3 in Section S.2 of the Supplementary Material.

Assumption 4.4. *There exists a constant $c \in (0, 1/2]$ such that $c \leq P(D = 1) \leq 1 - c$.*

Assumption 4.4 is the standard overlap condition in the DID literature, ensuring that both treated and untreated groups have a positive minimum population fraction.

Theorem 4.1. *Under Assumptions 3.1–4.4 it holds for the estimate $\hat{\tau}$ of the GATT that*

$$d_{\mathcal{G}}(\hat{\tau}, \tau) = O_p(n^{-1/2(\kappa-1)}).$$

For the example spaces in Examples 1–3 one has $\kappa = 2$, yielding the parametric convergence rate $O_p(n^{-1/2})$.

5 Implementation and Simulations

5.1 Implementation details and simulation scenarios

The proposed algorithm is outlined in Algorithm 1. The first step involves calculating Fréchet means. For Example 1, due to the convexity of the Wasserstein space, this reduces to the mean of quantile functions. For Example 3, it simplifies to the entry-wise mean of matrices. The Fréchet mean for Example 2 can be computed using the R package `manifold` (Dai et al., 2021). The second step involves constructing the geodesic transport map, with details provided in Section S.1 of the Supplementary Material.

Algorithm 1: Geodesic Difference-in-Differences

Input: data $\{(Y_{i,0}, Y_{i,1}, D_i)\}_{i=1}^n$.

Output: Difference-in-differences estimator of the Geodesic Average Treatment effect on the Treated (GATT) τ .

- 1 $(\hat{\nu}_{0,0}, \hat{\nu}_{0,1}, \hat{\nu}_{1,0}, \hat{\nu}_{1,1}) \leftarrow$ the estimated Fréchet means for the control and treated groups during pre- and post-treatment periods:

$$\hat{\nu}_{0,t} = \arg \min_{\omega \in \mathcal{M}} \frac{1}{n_0} \sum_{i=1}^n (1 - D_i) d^2(Y_{i,t}, \omega),$$

$$\hat{\nu}_{1,t} = \arg \min_{\omega \in \mathcal{M}} \frac{1}{n_1} \sum_{i=1}^n D_i d^2(Y_{i,t}, \omega),$$

where $t \in \{0, 1\}$;

- 2 $\hat{\nu}'_{1,1} = \Gamma_{\hat{\nu}_{0,0}, \hat{\nu}_{0,1}}(\hat{\nu}_{1,0}) \leftarrow$ the new end point of the geodesic $\gamma_{\hat{\nu}_{0,0}, \hat{\nu}_{0,1}}$ after moving to $\hat{\nu}_{1,0}$;
 - 3 $\hat{\tau} = \gamma_{\hat{\nu}'_{1,1}, \hat{\nu}_{1,1}} \leftarrow$ the difference-in-differences estimator of the GATT.
-

To evaluate the performance of the proposed approach, we report simulation results for various settings, specifically for the Wasserstein space and the space of networks equipped with the Frobenius metric (Examples 1 and 3). In all simulations, the group indicator D_i follows a Bernoulli distribution with parameter 0.25, i.e., $P(D_i = 1) = 0.25$.

We consider sample sizes $n = 50, 200, 1000$, with $Q = 500$ Monte Carlo runs. For the

q th Monte Carlo run, denote the GATT estimator by $\hat{\tau}_q$. The estimation quality for the q th run is assessed using the estimation error $d_{\mathcal{G}}(\hat{\tau}_q, \tau)$, where $d_{\mathcal{G}}$ is the geodesic distance as per (7), with the reference point chosen as $\nu'_{1,1}$.

5.2 Distributions

Consider the Wasserstein space described in Example 1, where the outcomes $Y_{i,0}$ and $Y_{i,1}$ are distributions. The quantile function for each outcome is generated as $F_{Y_{i,t}}^{-1} = \mu_{i,t} + \sigma_{i,t}\Phi^{-1}(\cdot)$ where $\mu_{i,t} \sim N(\alpha_2 t, 1)$, $\sigma_{i,t} = \alpha_1 + \beta D_i t$ and $\Phi^{-1}(\cdot)$ is the quantile function of the standard normal distribution. The parameters are set as $\alpha_1 = \alpha_2 = \beta = 1$.

As discussed in Section S.1 of the Supplementary Material, the geodesic transport map in the Wasserstein space corresponds to the optimal transport map. The starting point of the GATT $\tau = \gamma_{\nu'_{1,1}, \nu_{1,1}}$ is therefore $F_{\nu'_{1,1}}^{-1} = F_{\nu_{0,1}}^{-1} \circ F_{\nu_{0,0}} \circ F_{\nu_{1,0}}^{-1}$, where the quantile functions are $F_{\nu_{0,t}}^{-1} = \alpha_2 t + \alpha_1 \Phi^{-1}(\cdot)$, $F_{\nu_{1,t}}^{-1} = \alpha_2 t + (\alpha_1 + \beta t)\Phi^{-1}(\cdot)$. To simulate practical scenarios where the underlying distributions are almost always unknown and only independent data samples drawn from the distributions are available, we independently sample 100 observations from each distribution $Y_{i,t}$. The resulting empirical measures, which approximate the true but unknown distributions, are then used in the geodesic DID model. This approximation introduces an additional bias (Zhou and Müller, 2024).

The simulation results are shown in the left panel of Figure 2. As the sample size increases, the estimation error decreases, demonstrating the convergence of the estimated GATT to the target. The proposed geodesic DID model performs robustly, even in the presence of the aforementioned approximation bias. To evaluate the empirical rate of convergence, we fit a least-squares regression line to the log-transformed average estimation error versus $\log n$. For the Wasserstein space, the slope of the regression line is expected to

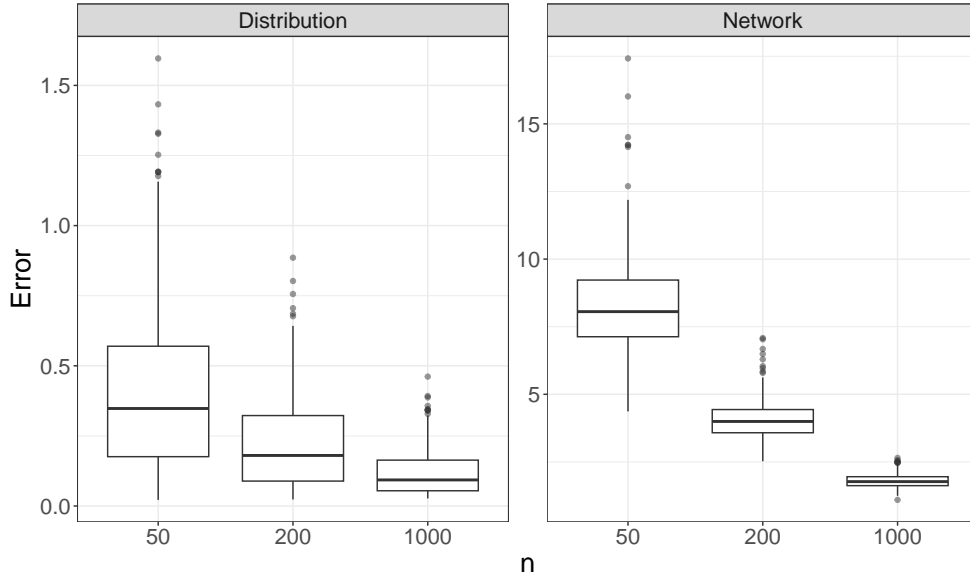


Figure 2: Boxplots of estimation errors with different sample sizes for distributions (left) and networks (right).

be approximately -0.5 . The observed slope from the simulations is -0.412 , suggesting a slightly slower empirical rate of convergence, likely due to the approximation error incurred by using empirical measures in lieu of the unknown distributions.

5.3 Networks

Consider the space of networks described in Example 3. Here the outcomes $Y_{i,0}$ and $Y_{i,1}$ are graph Laplacians, which are $m \times m$ symmetric, centered matrices (Zhou and Müller, 2022). We model the networks using a weighted stochastic block model with a community membership vector $\mathbf{z} = (\mathbf{z}_1, \mathbf{z}_2)'$ where \mathbf{z}_i is a vector of length m_i with all elements equal to i for $i = 1, 2$ and $m_1 + m_2 = m$. The existence of an edge between nodes within or across blocks is governed by a Bernoulli distribution, parameterized by the corresponding entry in the edge probability matrix $\begin{pmatrix} p_{11} & p_{12} \\ p_{21} & p_{22} \end{pmatrix}$. The weights of existing edges are independently generated as $\alpha_1 + \alpha_2 t + \alpha_3 D_i + \beta D_i t + \epsilon_i$, where $\alpha_1 = \alpha_2 = \alpha_3 = \beta = 1$, and the noise ϵ_i is independently sampled from a uniform distribution on $[-1, 1]$. The graph Laplacian

associated with each network is then used as the outcome.

The goal is to estimate the GATT $\tau = \gamma_{\nu'_{1,1}, \nu_{1,1}}$, where $\nu_{d,t} = E_{\oplus}(Y_{i,t} | D_i = d)$ and $\nu'_{1,1} = \Gamma_{\nu_{0,0}, \nu_{0,1}}(\nu_{1,0}) = \nu_{1,0} + (\nu_{0,1} - \nu_{0,0})$; see Section S.1 of the Supplementary Material. Using $(\nu_{d,t})_{jk}$ to denote the (j, k) th entry of the graph Laplacian $\nu_{d,t}$, under the Frobenius norm, we have

$$(\nu_{0,t})_{jk} = -p_{ll'}(\alpha_1 + \alpha_2 t), \quad (\nu_{1,t})_{jk} = -p_{ll'}(\alpha_1 + \alpha_2 t + \alpha_3 + \beta t)$$

for $1 \leq j \neq k \leq m$, where $l, l' \in \{1, 2\}$ represent the community memberships of nodes j and k , respectively. The diagonal entries of $\nu_{d,t}$ are $(\nu_{d,t})_{jj} = -\sum_{k \neq j} (\nu_{d,t})_{jk}$.

The right panel of Figure 2 presents the simulation results for networks with $m_1 = m_2 = 5, p_{11} = p_{22} = 0.5$ and $p_{12} = p_{21} = 0.2$. The estimation error decreases as the sample size increases, demonstrating the convergence of the estimated GATT to the target value. Similar to the analysis in subsection 5.2, we fit a least-squares regression line to the log-transformed average estimation error versus $\log n$. The observed slope of -0.509 aligns closely with the theoretical expectation of -0.5 , validating our theoretical framework.

6 Data Applications

6.1 Impact of the collapse of the Soviet Union on age-at-death distributions

The collapse of the Soviet Union in 1991 profoundly affected population dynamics, with dramatic declines in life expectancy observed across many former Soviet states. In Russia alone, life expectancy at birth between 1990 and 1994 dropped significantly by 6.2 years for men (from 63.8 to 57.6) and by 3.4 years for women (from 74.4 to 71.0) (Leon et al., 1997). Similar patterns were observed in other former Soviet states (Brainerd and Cutler,

Table 1: Six Eastern European countries that were part of the former Soviet Union and 19 Western European countries.

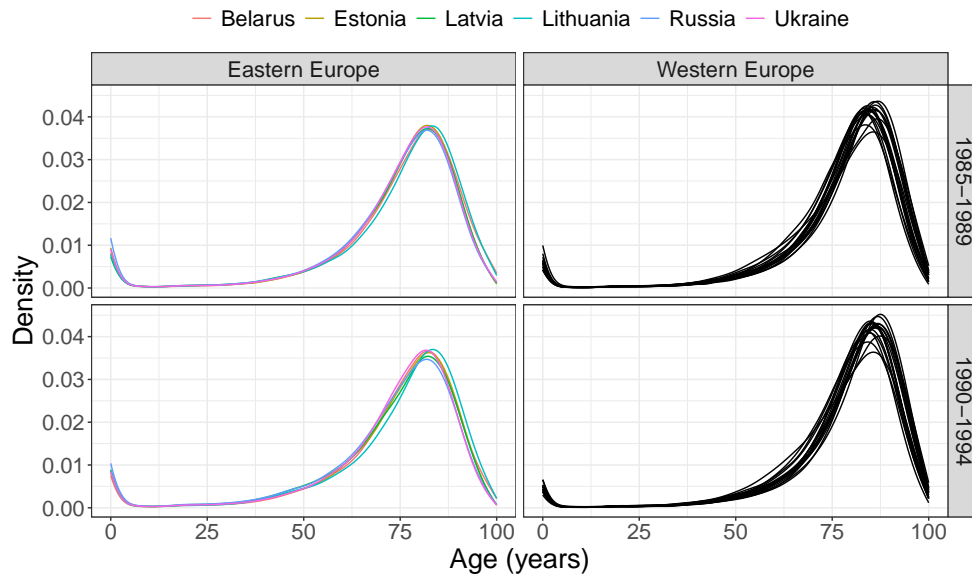
Eastern Europe	Belarus, Estonia, Latvia, Lithuania, Russia, Ukraine
Western Europe	Austria, Belgium, Denmark, Finland, France, Germany, Greece, Iceland, Ireland, Italy, Luxembourg, Netherlands, Norway, Portugal, Slovenia, Spain, Sweden, Switzerland, United Kingdom

2005). Adopting the entire age-at-death distribution as outcome provides deeper insights into trends of human longevity. To study causal effects, we applied the proposed geodesic DID model with age-at-death distributions as the outcome.

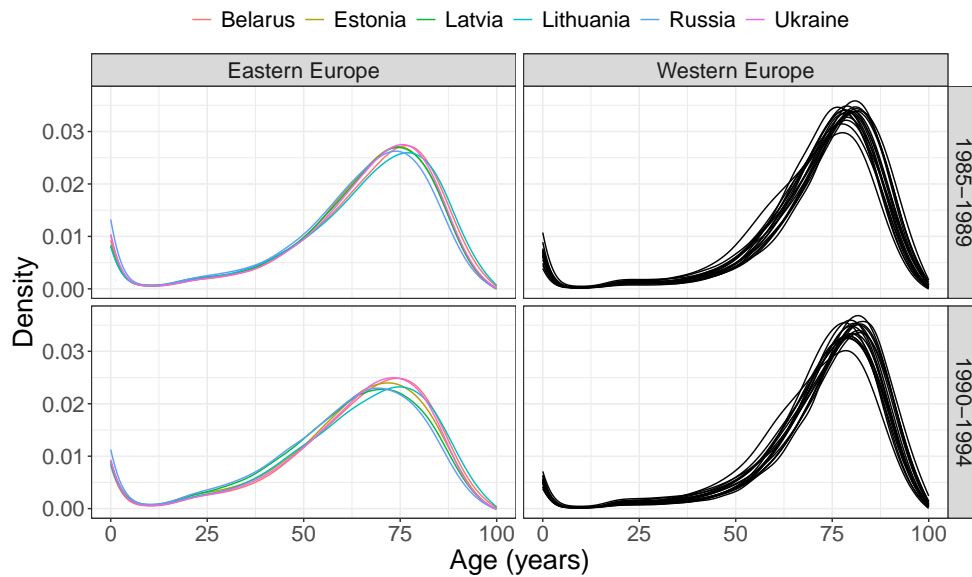
The Human Mortality Database (<http://www.mortality.org>) provides life tables at one-, five-, or ten-year intervals for various countries, including the six countries that were previously part of the former Soviet Union and 19 Western European countries. The six countries of the former Soviet Union form the intervention group, as they were subject to the collapse of the Soviet Union, while the 19 Western European countries serve as the control group. Further details of these groups are presented in Table 1.

For each country, the age-at-death distributions are derived from histograms of death counts by age, which are available in five-year intervals. These histograms are smoothed into continuous age-at-death densities using the `CreateDensity` function in the `frechet` package (Chen et al., 2023b). We analyze these densities for two time periods: 1985–1989 (before the collapse) and 1990–1994 (after the collapse). Figure 3 illustrates the densities of the age-at-death distributions for females and males in both intervention and control groups. In the intervention group, a clear leftward shift in the densities is observed for both genders, reflecting a reduction in life expectancy after the collapse. The shift is notably more pronounced for males.

Using the geodesic DID model, we estimate the GATT for age-at-death distributions. The estimated GATT for females and males is visualized in Figure 4. The results indicate



(a)



(b)

Figure 3: Age-at-death distributions of (a) females and (b) males for Eastern and Western European countries before and after the collapse of the Soviet Union.

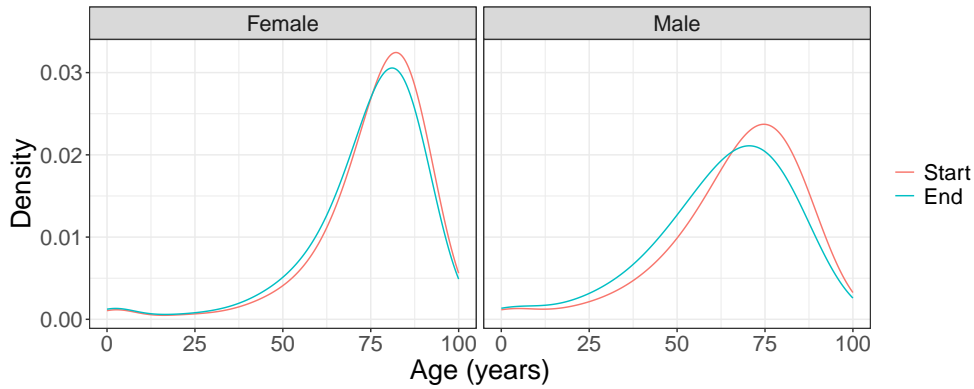


Figure 4: Estimated Geodesic Average Treatment Effect on the Treated (GATT) for age-at-death distributions of females (left) and males (right). The red curve represents the age-at-death densities at the starting point of the estimated GATT, while the blue curve represents the densities at the end point.

a causal effect of the Soviet Union’s collapse on age-at-death distributions, as evidenced by the differences between the start and end points of the geodesic that represents the estimate of GATT. For females, the age-at-death densities shift to the left, reflecting reduced life expectancy. For males, the effect is even stronger, which may be attributed to increased alcohol consumption and increased susceptibility of males to the social and economic instability during this period.

To validate the parallel trends assumption (Assumption 3.2), we compare age-at-death distributions for the periods 1980–1984 and 1985–1989, both of which precede the Soviet Union’s collapse. Figure 5 demonstrates that the age-at-death densities align closely for both genders during these periods, confirming that the parallel trends assumption holds in this application.

6.2 Impact of U.S. electricity market liberalization on electricity generation

We analyze U.S. electricity generation data, publicly available from the U.S. Energy Information Administration’s website (<https://www.eia.gov/electricity/data/state/>).

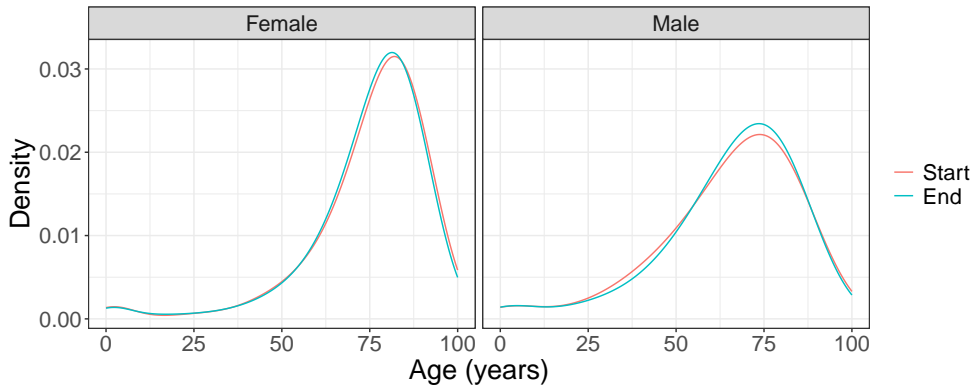


Figure 5: Verification of the parallel trends assumption by comparing age-at-death distributions between 1980–1984 and 1985–1989.

This dataset provides annual electricity generation figures by energy source for each state from 1990 to 2023. We consider the following three categories of energy sources: fossil (combining “coal” and “petroleum”), nuclear (corresponding solely to the “nuclear” category), and renewables (combining “hydroelectric conventional,” “solar thermal and photovoltaic,” “geothermal,” “wind,” and “wood and wood-derived fuels”). For each of the 50 states and each year, the share of electricity generation from each category is represented as a three-dimensional compositional vector. The component-wise square root transformation (see Example 2) then maps these compositional outcomes onto the positive quadrant of the sphere $\mathcal{S}_+^2 \subset \mathbb{R}^3$, which we endow with the geodesic metric.

In the early 1990s, the electricity system in the United States was dominated by vertically integrated monopoly utility companies, which controlled approximately 92% of electricity generation and consumption. This structure was supported under the “natural monopoly” argument: the economies of scale in infrastructure investment, combined with the network externalities of distribution systems, justified centralized control. Regulators required these monopolies to provide reliable electricity access at cost-based prices, an arrangement known as the “regulatory compact.” This model governed the electricity industry in the U.S. and many other countries for nearly a century (Joskow, 1997).

Table 2: 23 treated and 27 control states.

Treated states	Arizona, Arkansas, California, Connecticut, Delaware, Illinois, Maine, Maryland, Massachusetts, Montana, Nevada, New Hampshire, New Jersey, New Mexico, New York, Ohio, Oklahoma, Oregon, Pennsylvania, Rhode Island, Texas, Virginia, West Virginia
Control states	Alabama, Alaska, Colorado, Florida, Georgia, Hawaii, Idaho, Indiana, Iowa, Kansas, Kentucky, Louisiana, Michigan, Minnesota, Mississippi, Missouri, Nebraska, North Carolina, North Dakota, South Carolina, South Dakota, Tennessee, Utah, Vermont, Washington, Wisconsin, Wyoming

The 1992 National Energy Policy Act initiated changes that challenged this traditional system by promoting competition in electricity generation. These efforts culminated in 1996 with the issuance of Federal Energy Regulatory Commission (FERC) Order 888, which prohibited utilities from leveraging their control of transmission infrastructure to favor their own generators. This eliminated a significant barrier to entry for third-party electricity producers. However, states retained the authority to decide whether to implement these reforms (Joskow, 1997). Between 1996 and 2000, 23 states adopted electricity market liberalization through legislation, forming the treated group, while the remaining 27 states, which did not enact such changes, serve as the control group (see Table 2).

The objective of this analysis is to assess the causal effect of electricity market liberalization on the composition of energy sources used for electricity generation. For this purpose, we use 1995, the year prior to market liberalization, as the pre-treatment period, and 2020, 25 years later, as the post-treatment period. This long post-treatment period accounts for the gradual influence of market liberalization (Lee, 2020). Figures 6 and 7 depict the compositions of energy sources for electricity generation for both the treated and control groups, using sphere and ternary plots, respectively. For the treated states, a distinct upward-rightward trend is observed in the composition in Figure 6, reflecting a decline in fossil fuels and an increase in nuclear energy and renewables after market liberalization.

Using the geodesic DID model, we estimate the GATT for these compositional outcomes.

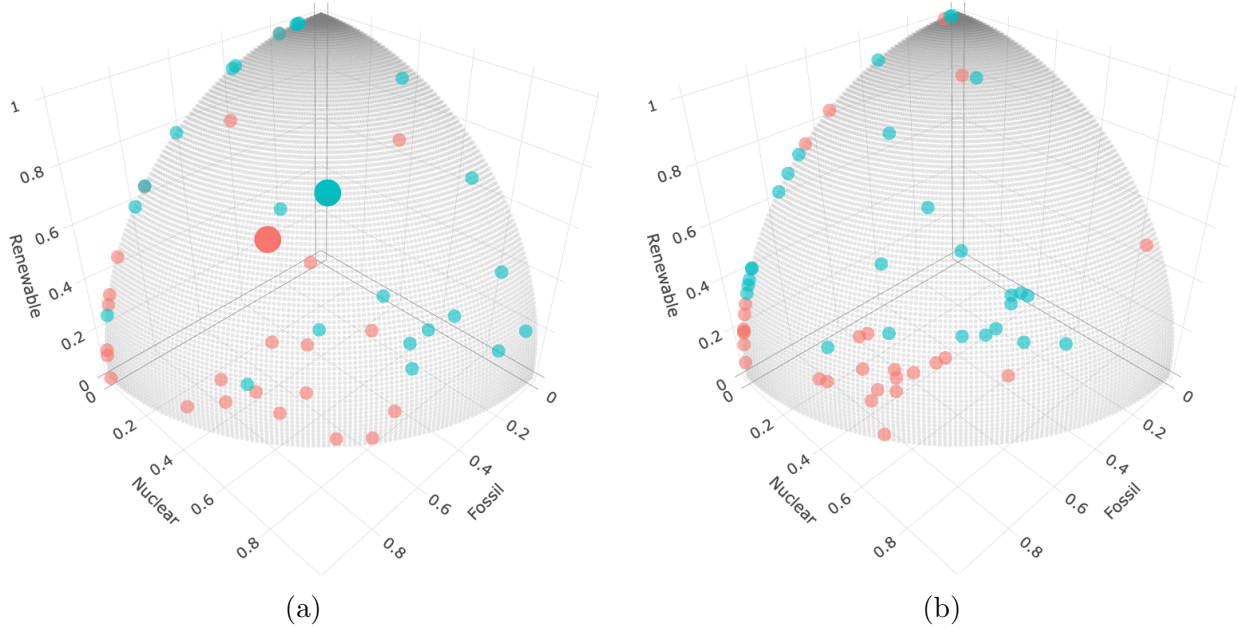


Figure 6: Compositions of energy sources for electricity generation for (a) treated and (b) control states. The red and blue dots represent compositions before and after the electricity market liberalization. The two larger dots correspond to the start (red) and end (blue) points of the estimated GATT.

The estimate is visualized in the left panels of Figures 6 and 7. The starting and ending compositions of the estimated GATT are $(0.432, 0.195, 0.373)'$ and $(0.231, 0.255, 0.514)'$, respectively. The results demonstrate a causal effect of electricity market liberalization on the composition of energy sources for electricity generation. Specifically, renewable energy sources gained a larger share following market liberalization, while the share of fossil fuels declined. These findings suggest that deregulation incentivized cleaner energy practices and supported a transition toward more sustainable energy systems.

To evaluate the validity of the parallel trends assumption, we compare compositional outcomes for the periods 1990 and 1995. The year 1990 is selected as the earliest available data point for the energy dataset. For this comparison, the starting composition of the estimated GATT is $(0.694, 0.181, 0.125)'$, and the ending composition is $(0.685, 0.179, 0.136)'$. The small size of the changes between these periods indicates that the parallel trends

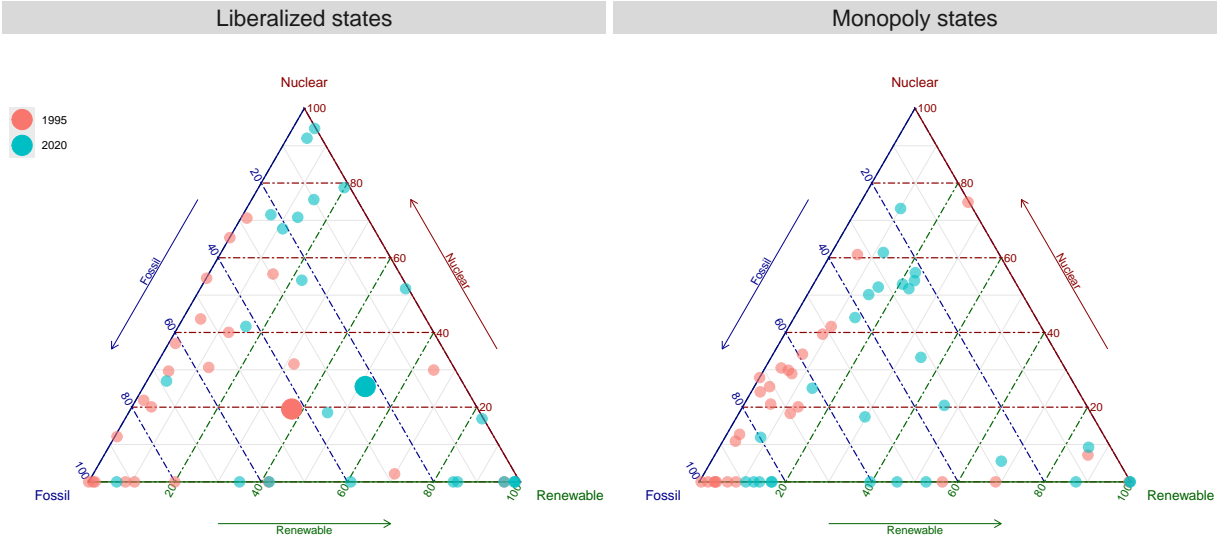


Figure 7: Ternary plots illustrating compositions of energy sources for electricity generation for treated (left) and control (right) states. The red and blue dots represent compositions before and after the electricity market liberalization. The two larger dots correspond to the start (red) and end (blue) points of the estimated GATT.

assumption approximately applies, ensuring the validity of the geodesic DID model.

7 Extension to the staggered case

7.1 Geodesic staggered DID

The staggered case features multiple time periods and variations in treatment timing. The theoretical results provided in this section can be seen as a natural extension of those in [Callaway and Sant’Anna \(2021\)](#) for Euclidean data to the case of outcomes in unique geodesic spaces. We introduce notations similar to those in [Callaway and Sant’Anna \(2021\)](#). Let $D_{i,t}$ be a binary variable equal to one if unit $i \in \{1, \dots, n\}$ is treated in period $t \in \{0, 1, \dots, T\}$ and equal to zero otherwise, where we require

Assumption 7.1 (Irreversibility of Treatment). *For any unit $i = 1, \dots, n$,*

(i) $D_{i,0} = 0$;

(ii) if $D_{i,t-1} = 1$, then $D_{i,t} = 1$ for $t = 1, \dots, T$.

Assumption 7.1 means that every unit is untreated at time $t = 0$ and that once a unit becomes treated, the unit will remain treated in the following periods. This assumption is commonly referred to as staggered treatment adoption.

Let G_i denote the time period when unit i first becomes treated. If a unit does not become treated in any time period, we set $G_i = \infty$. For all units that are treated, G_i indicates which “group” unit i belongs to. Let $G_{i,g}$ denote a binary variable i.e. equal to one if unit i is first treated in period g , i.e., $G_{i,g} = 1\{G_i = g\}$, and C_i denote a binary variable i.e. equal to one if unit i does not participate in the treatment in any time period, i.e., $C_i = 1\{G_i = \infty\} = 1 - D_{i,T}$.

For the observed outcome $Y_{i,t} \in \mathcal{M}$ for each unit i at time t , we assume

$$Y_{i,t} = \begin{cases} Y_{i,t}(0) & \text{if } C_i = 1, \\ Y_{i,t}(g) & \text{if } C_i = 0, G_{i,g} = 1, \end{cases}$$

where $Y_{i,t}(0)$ denotes unit i 's untreated potential outcome at time t if the unit remains untreated through time period T , i.e., if it is never treated across all available time periods and $Y_{i,t}(g)$ denotes the potential outcome for unit i at time t if the unit was to first become treated in time period $g = 1, \dots, T$. Assume that $\{(Y_{i,0}, Y_{i,1}, \dots, Y_{i,T}, D_{i,0}, D_{i,1}, \dots, D_{i,T})\}_{i=1}^n$ is an i.i.d. sample drawn from a joint distribution P , where a generic random variable distributed according to P is $(Y_0, Y_1, \dots, Y_T, D_0, D_1, \dots, D_T)$, where $Y_t \in \mathcal{M}$ and $D_t \in \{0, 1\}$, $t = 0, \dots, T$. Now we define the following notion of causal effects under the staggered treatment adoption.

Definition 7.1 (Group-Time GATT). *The geodesic average treatment effect for units who are members of a group g at a time period t is defined as the geodesic connecting*

$E_{\oplus}(Y_{i,t}(0)|G_{i,g} = 1)$ and $E_{\oplus}(Y_{i,t}(g)|G_{i,g} = 1)$, i.e., $\tau(g, t) = \gamma_{E_{\oplus}(Y_{i,t}(0)|G_{i,g}=1), E_{\oplus}(Y_{i,t}(g)|G_{i,g}=1)}$.

We refer to $\tau(g, t)$ as the group-time GATT of a group g at a time period t .

7.2 Identification

In this subsection, we provide results for the identification of the group-time GATT $\tau(g, t)$.

Let $\tilde{\mathcal{G}}$ denote the support of $\{G_i\}_{i=1}^n$. We set $\bar{g} = \max_{1 \leq i \leq n} G_i$ if $G_i \leq T$ for all i and $\bar{g} = \infty$ if $G_i = \infty$ for some i . Define $\mathcal{G} = \tilde{\mathcal{G}} \setminus \{\bar{g}\} \subset \{1, 2, \dots, T\}$. We require

Assumption 7.2 (Limited Treatment Anticipation). *There is a known $\delta \geq 0$ such that*

$$E_{\oplus}(Y_{i,t}(g)|G_{i,g} = 1) = E_{\oplus}(Y_{i,t}(0)|G_{i,g} = 1)$$

for all $g \in \mathcal{G}$, $t \in \{0, 1, \dots, T\}$ with $t < g - \delta$.

Assumption 7.3 (Parallel Trends Assumption based on a Never-Treated Group). *Let δ be as defined in Assumption 7.2. For each $g \in \mathcal{G}$ and $t \in \{1, \dots, T\}$ such that $t \geq g - \delta$,*

$$\Gamma_{\alpha, \beta}(E_{\oplus}(Y_{i,t-1}(0)|G_{i,g} = 1)) = E_{\oplus}(Y_{i,t}(0)|G_{i,g} = 1),$$

where $\alpha = E_{\oplus}(Y_{i,t-1}(0)|C_i = 1)$ and $\beta = E_{\oplus}(Y_{i,t}(0)|C_i = 1)$.

Assumption 7.4 (Parallel Trends Assumption based on a Not-Yet-Treated Group). *Let δ be as defined in Assumption 7.2. For each $g \in \mathcal{G}$ and each $(s, t) \in \{1, \dots, T\} \times \{1, \dots, T\}$ such that $t \geq g - \delta$ and $t + \delta \leq s < \bar{g}$,*

$$\Gamma_{\alpha, \beta}(E_{\oplus}(Y_{i,t-1}(0)|G_{i,g} = 1)) = E_{\oplus}(Y_{i,t}(0)|G_{i,g} = 1),$$

where $\alpha = E_{\oplus}(Y_{i,t-1}(0)|D_{i,s} = 0, G_{i,g} = 0)$ and $\beta = E_{\oplus}(Y_{i,t}(0)|D_{i,s} = 0, G_{i,g} = 0)$.

Assumption 7.2 restricts anticipation of the treatment for all treated groups. When $\delta = 0$, it corresponds to a “no-anticipation” assumption. Assumptions 7.3 and 7.4 restrict

the evolution of untreated potential outcomes and these are generalizations of the parallel trends assumption (Assumption 3.2). Assumption 7.3 means that the average outcomes for the group first treated in period g and for the “never-treated” group have parallel paths in the absence of treatment. Assumption 7.4 imposes parallel trends between group g and “not-yet-treated” groups by time $t + \delta$. For further discussion of Assumptions 7.3 and 7.4 for the Euclidean special case we refer to Callaway and Sant’Anna (2021).

For a generic $\delta \geq 0$, define $\mathcal{G}_\delta = \mathcal{G} \cap \{1 + \delta, 2 + \delta, \dots, T + \delta\}$. As we will see in Theorem 7.1, we can identify the group-time GATT $\tau(g, t)$. Figure 8 illustrates the identification of the group-time GATT using geodesic transport maps.

Theorem 7.1. *Suppose that Assumptions 3.1, 7.1 and 7.2 hold.*

(i) *If Assumption 7.3 holds, then for all g and t such that $g \in \mathcal{G}_\delta$, $t \in \{1, \dots, T - \delta\}$ and $t \geq g - \delta$, we have $\tau(g, t) = \gamma_{\beta_t, E_\oplus(Y_{i,t}|G_{i,g}=1)}$, where β_t is defined recursively as*

$$\beta_s = \begin{cases} E_\oplus(Y_{i,g-\delta-1}|G_{i,g} = 1) & s = g - \delta - 1, \\ \Gamma_{E_\oplus(Y_{i,s-1}|C_i=1), E_\oplus(Y_{i,s}|C_i=1)}(\beta_{s-1}) & s = \min\{g - \delta, t - 1\}, \dots, t. \end{cases}$$

(ii) *If Assumption 7.4 holds, then for all g and t such that $g \in \mathcal{G}_\delta$, $t \in \{1, \dots, T - \delta\}$ and $g - \delta \leq t < \bar{g} - \delta$, we have $\tau(g, t) = \gamma_{\beta_t, E_\oplus(Y_{i,t}|G_{i,g}=1)}$, where β_t is defined recursively as*

$$\beta_s = \begin{cases} E_\oplus(Y_{i,g-\delta-1}|G_{i,g} = 1) & s = g - \delta - 1, \\ \Gamma_{\nu_{s-1}, \nu_s}(\beta_{s-1}) & s = \min\{g - \delta, t - 1\}, \dots, t, \end{cases}$$

with $\nu_s = E_\oplus(Y_{i,s}|D_{i,t+\delta} = 0, G_{i,g} = 0)$.

The identification results in Theorem 7.1 become more concise if we additionally assume the following condition:

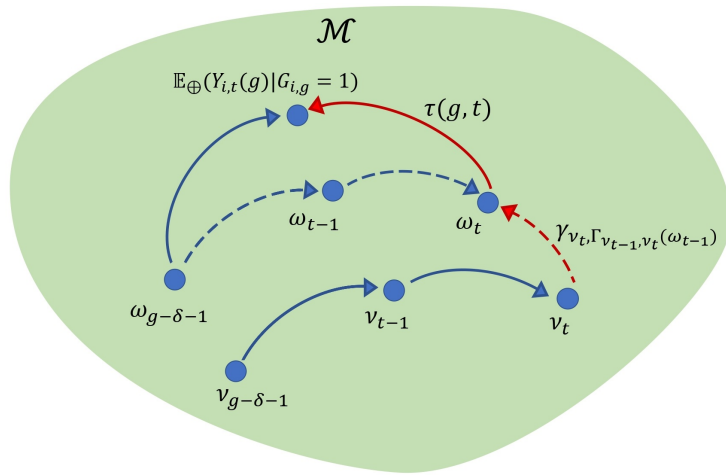


Figure 8: Illustration of geodesic staggered DID. The blue solid circles symbolize objects in the unique geodesic space \mathcal{M} . The arrows emanating from the circles represent the geodesic paths connecting them. The red arrows represent the geodesic transport from ν_t to ω_t and the proposed group-time GATT. Here, $\omega_s = E_{\oplus}(Y_{i,s}(0)|G_{i,g} = 1)$. Under Assumption 7.3, we set $\nu_s = E_{\oplus}(Y_{i,s}(0)|C_i = 1)$. Under Assumptions 7.4, we set $\nu_s = E_{\oplus}(Y_{i,s}(0)|D_{i,t+\delta} = 0, G_{i,g} = 0)$.

Assumption 7.5. For any $\alpha, \beta, \zeta, \omega \in \mathcal{M}$ with $\alpha \neq \beta$,

$$(\Gamma_{\zeta, \beta} \circ \Gamma_{\alpha, \zeta})(\omega) := \Gamma_{\zeta, \beta}(\Gamma_{\alpha, \zeta}(\omega)) = \Gamma_{\alpha, \beta}(\omega).$$

Assumption 7.5 imposes a consistency condition on the geodesic transport map, ensuring that transporting via an intermediate point ζ is equivalent to direct transport from α to β . This path-independence simplifies the analysis of geodesic operations within the DID framework. The assumption naturally holds in spaces such as Euclidean spaces, the Wasserstein space, the space of networks, and the space of covariance matrices.

Corollary 7.1. Suppose that Assumptions 3.1, 7.1, 7.2 and 7.5 hold.

- (i) If Assumption 7.3 holds, then for all g and t such that $g \in \mathcal{G}_\delta$, $t \in \{1, \dots, T - \delta\}$ and $t \geq g - \delta$, we have

$$\tau(g, t) = \ominus \gamma_{E_{\oplus}(Y_{i,g-\delta-1}|C_i=1), E_{\oplus}(Y_{i,t}|C_i=1)} \oplus \gamma_{E_{\oplus}(Y_{i,g-\delta-1}|G_{i,g}=1), E_{\oplus}(Y_{i,t}|G_{i,g}=1)}.$$

(ii) If Assumption 7.4 holds, then for all g and t such that $g \in \mathcal{G}_\delta$, $t \in \{1, \dots, T - \delta\}$ and $g - \delta \leq t < \bar{g} - \delta$, we have

$$\tau(g, t) = \ominus \gamma_{E_\oplus(Y_{i,g-\delta-1}|D_{i,t+\delta}=0, G_{1,g}=0), E_\oplus(Y_{i,t}|D_{i,t+\delta}=0, G_{i,g}=0)} \oplus \gamma_{E_\oplus(Y_{i,g-\delta-1}|G_{i,g}=1), E_\oplus(Y_{i,t}|G_{i,g}=1)}.$$

7.3 Estimation

In this subsection, we discuss the estimation of the group-time GATT $\tau(g, t)$ under the parallel trends assumption for either a never-treated group (Assumption 7.3) or a not-yet-treated group (Assumption 7.4). The asymptotic properties of the estimators are not elaborated here, but can be established along the lines of Theorem 4.1. We first consider the estimation of $\tau(g, t)$ under Assumption 7.3. In this case, we can estimate $\tau(g, t)$ as $\hat{\tau}(g, t) = \gamma_{\hat{\beta}_t, \hat{\nu}_{1,t}}$ where

$$\hat{\beta}_s = \begin{cases} \hat{\nu}_{1,g-\delta-1} & s = g - \delta - 1, \\ \Gamma_{\hat{\nu}_{0,s-1}, \hat{\nu}_{0,s}}(\hat{\beta}_{s-1}) & s = \min\{g - \delta, t - 1\}, \dots, t, \end{cases}$$

$$\hat{\nu}_{0,s} = \operatorname{argmin}_{\omega \in \mathcal{M}} \frac{1}{n_{\text{nev}}} \sum_{i=1}^n C_i d^2(Y_{i,s}, \omega), \quad n_{\text{nev}} = \sum_{i=1}^n C_i,$$

$$\hat{\nu}_{1,s} = \operatorname{argmin}_{\omega \in \mathcal{M}} \frac{1}{n_g} \sum_{i=1}^n G_{i,g} d^2(Y_{i,s}, \omega), \quad n_g = \sum_{i=1}^n G_{i,g}.$$

If Assumption 7.5 additionally holds, then the estimator has the simpler form $\hat{\tau}(g, t) = \ominus \gamma_{\hat{\nu}_{0,g-\delta-1}, \hat{\nu}_{0,t}} \oplus \gamma_{\hat{\nu}_{1,g-\delta-1}, \hat{\nu}_{1,t}}$.

Next we consider the estimation of $\tau(g, t)$ under Assumption 7.4. In this case, we can estimate $\tau(g, t)$ as $\hat{\tau}(g, t) = \gamma_{\hat{\beta}_t, \hat{\nu}_{1,t}}$ where

$$\hat{\beta}_s = \begin{cases} \hat{\nu}_{1,g-\delta-1} & s = g - \delta - 1, \\ \Gamma_{\hat{\nu}_{0,s-1}, \hat{\nu}_{0,s}}(\hat{\beta}_{s-1}) & s = \min\{g - \delta, t - 1\}, \dots, t, \end{cases}$$

$$\begin{aligned}\hat{\nu}_{0,s} &= \operatorname{argmin}_{\omega \in \mathcal{M}} \frac{1}{n_{\text{ny}}} \sum_{i=1}^n (1 - D_{i,t+\delta})(1 - G_{i,g}) d^2(Y_{i,s}, \omega), \\ n_{\text{ny}} &= \sum_{i=1}^n (1 - D_{i,t+\delta})(1 - G_{i,g}), \\ \hat{\nu}_{1,s} &= \operatorname{argmin}_{\omega \in \mathcal{M}} \frac{1}{n_g} \sum_{i=1}^n G_{i,g} d^2(Y_{i,s}, \omega).\end{aligned}$$

If Assumption 7.5 additionally holds, then again the estimator has the simpler form $\hat{\tau}(g, t) =$

$$\ominus \gamma_{\hat{\nu}_{0,g-\delta-1}, \hat{\nu}_{0,t}} \oplus \gamma_{\hat{\nu}_{1,g-\delta-1}, \hat{\nu}_{1,t}}.$$

8 Concluding remarks

The proposed geodesic DID provides a general framework for investigating causal effects in observational studies with non-Euclidean outcomes, such as distributions, networks, and manifold-valued data, while also encompassing scalars and vectors as special cases. It is a very natural and seemingly canonical extension of the existing Euclidean framework of DID for outcomes in unique geodesic spaces. Despite the generality and broad applicability of this approach, several challenges remain. Inference for the causal estimand in standard DID has been well-studied under the assumption of independent sampling and extended to allow for serial correlation using clustering methods (Bertrand et al., 2004). However, these approaches cannot be directly applied to non-Euclidean outcomes due to the lack of linear structure and further research will be needed to address these and related issues.

Relaxing the parallel trends assumption, which has been explored for Euclidean settings (Abadie, 2005) is another promising future direction. In non-Euclidean spaces, parallel trends violations could be accommodated by extending the geodesic DID framework to incorporate model-based adjustments or alternative causal assumptions. This extension could enhance its applicability for scenarios where the parallel trends assumption does not hold. An extension to metric spaces that do not support geodesics and may not be length

spaces is another theoretical challenge for future exploration.

References

- Abadie, A. (2005) Semiparametric difference-in-differences estimators. *The Review of Economic Studies*, **72**, 1–19.
- Angrist, J. D. and Pischke, J.-S. (2009) *Mostly Harmless Econometrics: An Empiricist's Companion*. Princeton University Press.
- Antonakis, J., Bendahan, S., Jacquart, P. and Lalive, R. (2010) On making causal claims: A review and recommendations. *Leadership Quarterly*, **21**, 1086–1120.
- Athey, S. and Imbens, G. W. (2006) Identification and inference in nonlinear difference-in-differences models. *Econometrica*, **74**, 431–497.
- Ben-Michael, E., Feller, A. and Rothstein, J. (2022) Synthetic controls with staggered adoption. *Journal of the Royal Statistical Society Series B: Statistical Methodology*, **84**, 351–381.
- Bertrand, M., Duflo, E. and Mullainathan, S. (2004) How much should we trust differences-in-differences estimates? *The Quarterly Journal of Economics*, **119**, 249–275.
- Biewen, M., Fitzenberger, B. and Rümmele, M. (2022) Using distribution regression difference-in-differences to evaluate the effects of a minimum wage introduction on the distribution of hourly wages and hours worked. *Working paper*, IZA Discussion Paper.
- Brainerd, E. and Cutler, D. M. (2005) Autopsy on an empire: understanding mortality in Russia and the former Soviet Union. *Journal of Economic Perspectives*, **19**, 107–130.
- Bridson, M. R. and Haefliger, A. (1999) *Metric Spaces of Non-Positive Curvature*. Grundlehren der mathematischen Wissenschaften. Springer Berlin, Heidelberg.
- Callaway, B. and Sant'Anna, P. H. (2021) Difference-in-differences with multiple time periods. *Journal of Econometrics*, **225**, 200–230.
- Card, D. and Krueger, A. B. (1994) Minimum wages and employment: A case study of the fast-food industry in New Jersey and Pennsylvania. *American Economic Review*, **84**, 772–793.
- Chen, Y., Lin, Z. and Müller, H.-G. (2023a) Wasserstein regression. *Journal of the American Statistical Association*, **118**, 869–882.
- Chen, Y., Zhou, Y., Chen, H., Gajardo, A., Fan, J., Zhong, Q., Dubey, P., Han, K., Bhattacharjee, S., Zhu, C., Iao, S. I., Kundu, P., Petersen, A. and Müller, H.-G. (2023b) *frechet: Statistical Analysis for Random Objects and Non-Euclidean Data*. URL: <https://CRAN.R-project.org/package=frechet>. R package version 0.3.0.
- Dai, X., Lin, Z. and Müller, H.-G. (2021) Modeling sparse longitudinal data on Riemannian manifolds. *Biometrics*, **77**, 1328–1341.

- Ding, P. and Li, F. (2019) A bracketing relationship between difference-in-differences and lagged-dependent-variable adjustment. *Political Analysis*, **27**, 605–615.
- Dryden, I. L., Koloydenko, A. and Zhou, D. (2009) Non-Euclidean statistics for covariance matrices, with applications to diffusion tensor imaging. *Annals of Applied Statistics*, **3**, 1102–1123.
- Gunsilius, F. F. (2023) Distributional synthetic controls. *Econometrica*, **91**, 1105–1117.
- Joskow, P. L. (1997) Restructuring, competition and regulatory reform in the US electricity sector. *Journal of Economic Perspectives*, **11**, 119–138.
- Keele, L. (2015) The statistics of causal inference: A view from political methodology. *Political Analysis*, **23**, 313–335.
- Kurusu, D., Zhou, Y., Otsu, T. and Müller, H.-G. (2024) Geodesic causal inference. *arXiv preprint arXiv:2406.19604*.
- Lee, N. R. (2020) When competition plays clean: How electricity market liberalization facilitated state-level climate policies in the United States. *Energy Policy*, **139**, 111308.
- Leon, D. A., Chenet, L., Shkolnikov, V. M., Zakharov, S., Shapiro, J., Rakhmanova, G., Vassin, S. and McKee, M. (1997) Huge variation in Russian mortality rates 1984–94: artefact, alcohol, or what? *The Lancet*, **350**, 383–388.
- Lin, Z., Kong, D. and Wang, L. (2023) Causal inference on distribution functions. *Journal of the Royal Statistical Society Series B: Statistical Methodology*, **85**, 378–398.
- Lin, Z. and Yao, F. (2019) Intrinsic Riemannian Functional data analysis. *Annals of Statistics*, **47**, 3533–3577.
- McCann, R. J. (1997) A convexity principle for interacting gases. *Advances in Mathematics*, **128**, 153–179.
- Nye, T. M., Tang, X., Weyenberg, G. and Yoshida, R. (2017) Principal component analysis and the locus of the Fréchet mean in the space of phylogenetic trees. *Biometrika*, **104**, 901–922.
- Opoku-Agyemang, K. A. (2023) Differences-in-differences on distribution functions for program evaluations. *Development Economics Paper Model Ten*.
- Panaretos, V. M. and Zemel, Y. (2020) *An Invitation to Statistics in Wasserstein Space*. Springer New York.
- Petersen, A. and Müller, H.-G. (2019) Fréchet regression for random objects with Euclidean predictors. *Annals of Statistics*, **47**, 691–719.
- Petersen, A., Zhang, C. and Kokoszka, P. (2022) Modeling probability density functions as data objects. *Econometrics and Statistics*, **21**, 159–178.
- Roth, J. and Sant’Anna, P. H. (2023) When is parallel trends sensitive to functional form? *Econometrica*, **91**, 737–747.

- Roth, J., Sant’Anna, P. H., Bilinski, A. and Poe, J. (2023) What’s trending in difference-in-differences? a synthesis of the recent econometrics literature. *Journal of Econometrics*, **235**, 2218–2244.
- Scealy, J. and Welsh, A. (2011) Regression for compositional data by using distributions defined on the hypersphere. *Journal of the Royal Statistical Society Series B: Statistical Methodology*, **73**, 351–375.
- (2014) Colours and cocktails: Compositional data analysis. *Australian & New Zealand Journal of Statistics*, **56**, 145–169.
- Sofer, T., Richardson, D. B., Colicino, E., Schwartz, J. and Tchetgen, E. J. T. (2016) On negative outcome control of unobserved confounding as a generalization of difference-in-differences. *Statistical Science*, **31**, 348–361.
- Sturm, K.-T. (2003) Probability measures on metric spaces of nonpositive curvature. *Heat Kernels and Analysis on Manifolds, Graphs, and Metric Spaces (Paris, 2002)*. *Contemp. Math.*, 338. *Amer. Math. Soc., Providence, RI*, **338**, 357–390.
- Torous, W., Gunsilius, F. and Rigollet, P. (2024) An optimal transport approach to estimating causal effects via nonlinear difference-in-differences. *Journal of Causal Inference*, **12**, 20230004.
- van der Vaart, A. and Wellner, J. (2023) *Weak Convergence and Empirical Processes: With Applications to Statistics*. Springer New York, 2nd edn.
- Varian, H. R. (2016) Causal inference in economics and marketing. *Proceedings of the National Academy of Sciences*, **113**, 7310–7315.
- Wing, C., Simon, K. and Bello-Gomez, R. A. (2018) Designing difference in difference studies: best practices for public health policy research. *Annual Review of Public Health*, **39**, 453–469.
- Xu, Y., Zhao, A. and Ding, P. (2024) Factorial difference-in-differences. *arXiv preprint arXiv:2407.11937*.
- Ye, T., Ertefaie, A., Flory, J., Hennessy, S. and Small, D. S. (2023) Instrumented difference-in-differences. *Biometrics*, **79**, 569–581.
- Yuan, Y., Zhu, H., Lin, W. and Marron, J. (2012) Local polynomial regression for symmetric positive definite matrices. *Journal of the Royal Statistical Society Series B: Statistical Methodology*, **74**, 697–719.
- Zhou, Y. and Müller, H.-G. (2022) Network regression with graph Laplacians. *Journal of Machine Learning Research*, **23**, 1–41.
- Zhou, Y. and Müller, H.-G. (2024) Wasserstein regression with empirical measures and density estimation for sparse data. *Biometrics*, **80**, ujae127.
- Zhu, C. and Müller, H.-G. (2023) Geodesic optimal transport regression. *arXiv preprint arXiv:2312.15376*.

SUPPLEMENTARY MATERIAL

S.1 Geodesic Transport Maps

In the Wasserstein space from Example 1, Assumption 3.1 is satisfied with the geodesic transport map $\Gamma_{\alpha,\beta} = F_\beta^{-1} \circ F_\alpha$, where F_α and F_β^{-1} are the cumulative distribution function of α and the quantile function of β , respectively. The resulting endpoint of the geodesic $\gamma_{\alpha,\beta}$ is given by $F_\zeta^{-1} = F_\beta^{-1} \circ F_\alpha \circ F_\omega^{-1}$, where F_ω^{-1} and F_ζ^{-1} denote the quantile functions of ω and ζ , respectively.

For the space of spherical data described in Example 2, the geodesic transport map can be interpreted as a rotation of the point ω along the geodesic determined by α and β . The tangent vector for the geodesic $\gamma_{\alpha,\beta}$ is given by $v_{\alpha,\beta} = \beta - (\alpha'\beta)\alpha$, whose magnitude and direction encode the geodesic length and directionality needed to move from α toward β along the sphere. The geodesic transport map is then defined as:

$$\Gamma_{\alpha,\beta}(\omega) = \text{Exp}_\omega\left(\theta \frac{v}{\|v\|}\right) = \cos(\theta)\omega + \sin(\theta) \frac{v}{\|v\|},$$

where $\theta = \arccos(\alpha'\beta)$ is the angle between α and β , $v = v_{\alpha,\beta} - (\omega'v_{\alpha,\beta})\omega$ is the projection of $v_{\alpha,\beta}$ onto the tangent space at ω , and $\text{Exp}_\omega(\theta v/\|v\|)$ denotes the exponential map at ω applied to the tangent vector $\theta v/\|v\|$.

This map $\Gamma_{\alpha,\beta}(\omega)$ moves the point ω along the geodesic connecting it to a new point determined by α and β , with the direction and distance dictated by the original geodesic $\gamma_{\alpha,\beta}$. The construction ensures that $\Gamma_{\alpha,\beta}(\omega)$ lies on the sphere and preserves the geodesic structure. Assumption 3.1 is satisfied with this geodesic transport map.

For the space of networks or covariance matrices equipped with the Frobenius metric, the geodesic corresponds to the line segment connecting the start and end points. Assumption 3.1 is satisfied for Example 3 with the geodesic transport map $\Gamma_{\alpha,\beta}(\omega) = \omega + (\beta - \alpha)$.

S.2 Verification of Model Assumptions

Proposition S1. *Consider the Wasserstein space $(\mathcal{W}, d_{\mathcal{W}})$ consisting of absolutely continuous probability measures on a closed interval $I \subset \mathbb{R}$ with finite second moments, equipped with the Wasserstein distance $d_{\mathcal{W}}$. Write the density function of $\mu \in \mathcal{W}$ as f_{μ} . If there exist constants $0 < l \leq L < \infty$ such that $l \leq f_{\mu}(x) \leq L$ for all $\mu \in \mathcal{W}$ and $x \in I$, then the Wasserstein space $(\mathcal{W}, d_{\mathcal{W}})$ satisfies Assumptions 4.1, 4.2, and 4.3.*

Proof. Since $l \leq f_{\mu}(x) \leq L$ for all $\mu \in \mathcal{W}$ and $x \in I$, the cumulative distribution function F_{μ} and its inverse, the quantile function F_{μ}^{-1} , are both Lipschitz continuous with constants L and $1/l$, respectively.

Verification of Assumption 4.1: We need to show that

$$\begin{aligned} & \left[\int_0^1 \{F_2^{-1} \circ F_1 \circ G^{-1}(p) - F_2^{-1} \circ F_1 \circ H^{-1}(p)\}^2 dp \right]^{1/2} \\ & \leq C_1 \left[\int_0^1 \{G^{-1}(p) - H^{-1}(p)\}^2 dp \right]^{1/2}. \end{aligned}$$

Using the Lipschitz continuity of F_2^{-1} and F_1 , we have:

$$\begin{aligned} & \int_0^1 \{F_2^{-1} \circ F_1 \circ G^{-1}(p) - F_2^{-1} \circ F_1 \circ H^{-1}(p)\}^2 dp \\ & \leq \frac{1}{l^2} \int_0^1 \{F_1 \circ G^{-1}(p) - F_1 \circ H^{-1}(p)\}^2 dp \\ & \leq \frac{L^2}{l^2} \int_0^1 \{G^{-1}(p) - H^{-1}(p)\}^2 dp. \end{aligned}$$

Thus, Assumption 4.1 holds with $C_1 = L/l$.

Verification of Assumption 4.2: We need to show that

$$\begin{aligned} & \left[\int_0^1 \{F_2^{-1} \circ F_1 \circ H^{-1}(p) - G_2^{-1} \circ G_1 \circ H^{-1}(p)\}^2 dp \right]^{1/2} \\ & \leq C_2 \left(\left[\int_0^1 \{F_1^{-1}(p) - G_1^{-1}(p)\}^2 dp \right]^{1/2} + \left[\int_0^1 \{F_2^{-1}(p) - G_2^{-1}(p)\}^2 dp \right]^{1/2} \right). \end{aligned}$$

Using a change of variable $p = H(x)$, the left-hand side becomes

$$\begin{aligned} & \left[\int_0^1 \{F_2^{-1} \circ F_1 \circ H^{-1}(p) - G_2^{-1} \circ G_1 \circ H^{-1}(p)\}^2 dp \right]^{1/2} \\ &= \left[\int_I \{F_2^{-1} \circ F_1(x) - G_2^{-1} \circ G_1(x)\}^2 h(x) dx \right]^{1/2}. \end{aligned}$$

Since $h(x) \leq L$, we have

$$\begin{aligned} & \left[\int_I \{F_2^{-1} \circ F_1(x) - G_2^{-1} \circ G_1(x)\}^2 h(x) dx \right]^{1/2} \\ & \leq \sqrt{L} \left[\int_I \{F_2^{-1} \circ F_1(x) - G_2^{-1} \circ G_1(x)\}^2 dx \right]^{1/2}. \end{aligned}$$

Using the triangle inequality

$$\begin{aligned} & |F_2^{-1} \circ F_1(x) - G_2^{-1} \circ G_1(x)| \\ & \leq |F_2^{-1} \circ F_1(x) - F_2^{-1} \circ G_1(x)| + |F_2^{-1} \circ G_1(x) - G_2^{-1} \circ G_1(x)|. \end{aligned}$$

Squaring both sides and integrating, we obtain

$$\begin{aligned} & \int_I \{F_2^{-1} \circ F_1(x) - G_2^{-1} \circ G_1(x)\}^2 dx \\ & \leq 2 \int_I \{F_2^{-1} \circ F_1(x) - F_2^{-1} \circ G_1(x)\}^2 dx \\ & \quad + 2 \int_I \{F_2^{-1} \circ G_1(x) - G_2^{-1} \circ G_1(x)\}^2 dx. \end{aligned}$$

Taking the square root of both sides, we find

$$\begin{aligned} & \left[\int_I \{F_2^{-1} \circ F_1(x) - G_2^{-1} \circ G_1(x)\}^2 dx \right]^{1/2} \\ & \leq \sqrt{2} \left[\int_I \{F_2^{-1} \circ F_1(x) - F_2^{-1} \circ G_1(x)\}^2 dx \right]^{1/2} \\ & \quad + \sqrt{2} \left[\int_I \{F_2^{-1} \circ G_1(x) - G_2^{-1} \circ G_1(x)\}^2 dx \right]^{1/2}. \end{aligned}$$

For the first term, the Lipschitz continuity of F_2^{-1} ensures that

$$|F_2^{-1} \circ F_1(x) - F_2^{-1} \circ G_1(x)| \leq \frac{1}{l} |F_1(x) - G_1(x)|,$$

which implies:

$$\int_I \{F_2^{-1} \circ F_1(x) - F_2^{-1} \circ G_1(x)\}^2 dx \leq \frac{1}{l^2} \int_I \{F_1(x) - G_1(x)\}^2 dx.$$

Changing variables with $p = G_1(x)$, we rewrite

$$\int_I \{F_1(x) - G_1(x)\}^2 dx = \int_0^1 \{F_1 \circ G_1^{-1}(p) - p\}^2 \frac{1}{g_1 \circ G_1^{-1}(p)} dp.$$

Since $g_1(x) \geq l$, it follows that:

$$\int_0^1 \{F_1 \circ G_1^{-1}(p) - p\}^2 \frac{1}{g_1 \circ G_1^{-1}(p)} dp \leq \frac{1}{l} \int_0^1 \{F_1 \circ G_1^{-1}(p) - p\}^2 dp.$$

Using $p = F_1 \circ F_1^{-1}(p)$ and the Lipschitz continuity of F_1 (constant L):

$$\begin{aligned} \int_0^1 \{F_1 \circ G_1^{-1}(p) - p\}^2 dp &= \int_0^1 \{F_1 \circ G_1^{-1}(p) - F_1 \circ F_1^{-1}(p)\}^2 dp \\ &\leq L^2 \int_0^1 \{F_1^{-1}(p) - G_1^{-1}(p)\}^2 dp. \end{aligned}$$

Combining terms, we conclude

$$\int_I \{F_2^{-1} \circ F_1(x) - F_2^{-1} \circ G_1(x)\}^2 dx \leq \frac{L^2}{l^3} \int_0^1 \{F_1^{-1}(p) - G_1^{-1}(p)\}^2 dp.$$

For the second term, changing variables with $p = G_1(x)$, we have

$$\begin{aligned} \int_I \{F_2^{-1} \circ G_1(x) - G_2^{-1} \circ G_1(x)\}^2 dx &= \int_0^1 \{F_2^{-1}(p) - G_2^{-1}(p)\}^2 dG_1^{-1}(p) \\ &= \int_0^1 \{F_2^{-1}(p) - G_2^{-1}(p)\}^2 \frac{1}{g_1 \circ G_1^{-1}(p)} dp \\ &\leq \frac{1}{l} \int_0^1 \{F_2^{-1}(p) - G_2^{-1}(p)\}^2 dp. \end{aligned}$$

Combining the bounds for the first and second terms, we obtain

$$\begin{aligned} \left[\int_I \{F_2^{-1} \circ F_1(x) - G_2^{-1} \circ G_1(x)\}^2 dx \right]^{1/2} &\leq \sqrt{\frac{2L^2}{l^3}} \left[\int_0^1 \{F_1^{-1}(p) - G_1^{-1}(p)\}^2 dp \right]^{1/2} \\ &\quad + \sqrt{\frac{2}{l}} \left[\int_0^1 \{F_2^{-1}(p) - G_2^{-1}(p)\}^2 dp \right]^{1/2}. \end{aligned}$$

Finally, for the full expression, we have

$$\begin{aligned}
& \left[\int_0^1 \{F_2^{-1} \circ F_1 \circ H^{-1}(p) - G_2^{-1} \circ G_1 \circ H^{-1}(p)\}^2 dp \right]^{1/2} \\
& \leq \sqrt{L} \left[\int_I \{F_2^{-1} \circ F_1(x) - G_2^{-1} \circ G_1(x)\}^2 dx \right]^{1/2} \\
& \leq \sqrt{\frac{2L^3}{l^3}} \left[\int_0^1 \{F_1^{-1}(p) - G_1^{-1}(p)\}^2 dp \right]^{1/2} \\
& \quad + \sqrt{\frac{2L}{l}} \left[\int_0^1 \{F_2^{-1}(p) - G_2^{-1}(p)\}^2 dp \right]^{1/2}.
\end{aligned}$$

Thus, Assumption 4.2 is satisfied with $C_2 = (2L^3/l^3)^{1/2}$.

Verification of Assumption 4.3: Following the argument in Proposition 1 of [Petersen and Müller \(2019\)](#), one can verify that Assumption 4.3 holds with $C = 1$, $\kappa = 2$, and η arbitrary. \square

Proposition S2. *The space of compositional data $(\mathcal{S}_+^{d-1}, d_g)$ defined in Example 2 satisfies Assumptions 4.1, 4.2, and 4.3.*

Proof. Recall that the geodesic transport map $\Gamma_{\alpha,\beta}(\cdot)$ on $(\mathcal{S}_+^{d-1}, d_g)$, as defined in Section S.1 of the Supplementary Material, is given by:

$$\Gamma_{\alpha,\beta}(\omega) = \text{Exp}_\omega(\theta v) = \cos(\theta)\omega + \sin(\theta) \frac{v}{\|v\|},$$

where $\theta = \arccos(\alpha'\beta)$ is the angle between α and β and $v = v_{\alpha,\beta} - (\omega'v_{\alpha,\beta})\omega$ is the projection of $v_{\alpha,\beta}$ onto the tangent space at ω with $v_{\alpha,\beta} = \beta - (\alpha'\beta)\alpha$.

Verification of Assumption 4.1: We need to show that for any $\alpha, \beta, \omega, \zeta \in \mathcal{S}^{d-1}$, there exists a constant $C_1 > 0$ such that:

$$d_g(\Gamma_{\alpha,\beta}(\omega), \Gamma_{\alpha,\beta}(\zeta)) \leq C_1 d_g(\omega, \zeta).$$

Since $(\mathcal{S}_+^{d-1}, d_g)$ is bounded, it suffices to consider the case where ζ is a small perturbation of ω , so that their geodesic distance $d_g(\omega, \zeta)$ is small. The geodesic transport map $\Gamma_{\alpha, \beta}(\cdot)$ involves smooth operations such as cosine, sine, and projection, all of which are Lipschitz continuous on \mathcal{S}_+^{d-1} . Therefore, a small perturbation in ω results in a bounded proportional perturbation in $\Gamma_{\alpha, \beta}(\omega)$.

For the map $\Gamma_{\alpha, \beta}$ applied to ω and ζ , the Euclidean distance satisfies:

$$\|\Gamma_{\alpha, \beta}(\omega) - \Gamma_{\alpha, \beta}(\zeta)\| \leq C_1 \|\omega - \zeta\|,$$

where $C_1 > 0$ depends on $\alpha, \beta, \omega, \zeta$. Since the geodesic distance $d_g(\omega, \zeta)$ and the Euclidean distance $\|\omega - \zeta\|$ are locally equivalent metrics on \mathcal{S}_+^{d-1} , this inequality implies:

$$d_g(\Gamma_{\alpha, \beta}(\omega), \Gamma_{\alpha, \beta}(\zeta)) \leq C_1 d_g(\omega, \zeta).$$

Thus, Assumption 4.1 holds for the geodesic transport map, with a constant $C_1 > 0$ determined by the smoothness of the trigonometric and projection operations involved in the map.

Verification of Assumption 4.2: To verify this assumption, we need to show that for any $\alpha_1, \beta_1, \alpha_2, \beta_2, \omega \in \mathcal{S}^{d-1}$, there exists a constant $C_2 > 0$ such that

$$d_g(\Gamma_{\alpha_1, \beta_1}(\omega), \Gamma_{\alpha_2, \beta_2}(\omega)) \leq C_2 \{d_g(\alpha_1, \alpha_2) + d_g(\beta_1, \beta_2)\}.$$

It suffices to consider the case where α_2 and β_2 are small perturbations of α_1 and β_1 , respectively. From the definition of the geodesic transport map, the difference between $\Gamma_{\alpha_1, \beta_1}(\omega)$ and $\Gamma_{\alpha_2, \beta_2}(\omega)$ arises from two sources:

1. Differences in the geodesic angles, $\theta_1 = d_g(\alpha_1, \beta_1)$ and $\theta_2 = d_g(\alpha_2, \beta_2)$.
2. Differences in the tangent vectors, v_{α_1, β_1} and v_{α_2, β_2} .

Since α_2 and β_2 are close to α_1 and β_1 , respectively, these differences are small. Using the Lipschitz continuity of the trigonometric functions (cos and sin) and the projection operator, as well as the equivalence between the geodesic distance and the Euclidean distance on \mathcal{S}^{d-1} , we conclude

$$d_g(\Gamma_{\alpha_1, \beta_1}(\omega), \Gamma_{\alpha_2, \beta_2}(\omega)) \leq C_2 \{d_g(\alpha_1, \alpha_2) + d_g(\beta_1, \beta_2)\}.$$

Thus, Assumption 4.2 holds for the geodesic transport map $\Gamma_{\alpha, \beta}$, with the constant $C_2 > 0$ determined by the smoothness of the trigonometric and projection operations involved in the map.

Verification of Assumption 4.3: Using the approach outlined in Proposition 3 of [Petersen and Müller \(2019\)](#), it can be shown that Assumption 4.3 is satisfied with $\kappa = 2$. \square

Proposition S3. *The space of networks or space of covariance matrices (\mathcal{M}, d_F) defined in Example 3 satisfies Assumptions 4.1, 4.2, and 4.3.*

Proof. In the space of networks or space of covariance matrices equipped with the Frobenius metric, the geodesic is a simple line segment connecting the start and end points. This linear structure ensures that the geodesic transport map preserves distances exactly. Consequently, Assumptions 4.1 and 4.2 are satisfied with constants $C_1 = C_2 = 1$. Following the argument in Theorem 2 of [Zhou and Müller \(2022\)](#), one can verify that Assumption 4.3 holds with $C = 1$, $\kappa = 2$, and η arbitrary. \square

S.3 Proofs

S.3.1 Proof of Theorem 3.1

Proof. Observe that $\nu_{0,0}(0) = \nu_{0,0}$ and $\nu_{0,1}(0) = \nu_{0,1}$ since we observe $Y_{i,t}(0)$ directly for $t \in \{0,1\}$ for the control group. For the treated group, we likewise have $\nu_{1,0}(0) = \nu_{1,0}$ and $\nu_{1,1}(1) = \nu_{1,1}$. By Assumption 3.2 (parallel trends), we have $\Gamma_{\nu_{0,0},\nu_{0,1}}(\nu_{1,0}) = \Gamma_{\nu_{0,0}(0),\nu_{0,1}(0)}(\nu_{1,0}(0)) = \nu_{1,1}(0)$. It follows that

$$\ominus \gamma_{\nu_{0,0},\nu_{0,1}} \oplus \gamma_{\nu_{1,0},\nu_{1,1}} = \gamma_{\Gamma_{\nu_{0,0},\nu_{0,1}}(\nu_{1,0}),\nu_{1,1}} = \gamma_{\nu_{1,1}(0),\nu_{1,1}} = \gamma_{\nu_{1,1}(0),\nu_{1,1}(1)}.$$

□

S.3.2 Proof of Proposition 4.1

Proof. To show \sim is an equivalence relation on $\mathcal{G}(\mathcal{M})$, we verify the following properties:

- Reflexivity: $\gamma_{\alpha,\beta} \sim \gamma_{\alpha,\beta}$ for all $\gamma_{\alpha,\beta} \in \mathcal{G}(\mathcal{M})$.
- Symmetry: $\gamma_{\alpha_1,\beta_1} \sim \gamma_{\alpha_2,\beta_2}$ implies $\gamma_{\alpha_2,\beta_2} \sim \gamma_{\alpha_1,\beta_1}$ for all $\gamma_{\alpha_1,\beta_1}, \gamma_{\alpha_2,\beta_2} \in \mathcal{G}(\mathcal{M})$.
- Transitivity: if $\gamma_{\alpha_1,\beta_1} \sim \gamma_{\alpha_2,\beta_2}$ and $\gamma_{\alpha_2,\beta_2} \sim \gamma_{\alpha_3,\beta_3}$, then $\gamma_{\alpha_1,\beta_1} \sim \gamma_{\alpha_3,\beta_3}$ for all $\gamma_{\alpha_1,\beta_1}, \gamma_{\alpha_2,\beta_2}, \gamma_{\alpha_3,\beta_3} \in \mathcal{G}(\mathcal{M})$.

The property of reflexivity follows directly from the definition of the geodesic transport map in Assumption 3.1. The properties of symmetry and transitivity are satisfied by the definition of the relation \sim . □

S.3.3 Proof of Proposition 4.2

Proof. To demonstrate that the quotient space of geodesics $\mathcal{G}(\mathcal{M})/\sim$ is a metric space with the metric

$$d_{\mathcal{G}}([\gamma_{\alpha_1, \beta_1}], [\gamma_{\alpha_2, \beta_2}]) = d(\Gamma_{\alpha_1, \beta_1}(\omega_{\oplus}), \Gamma_{\alpha_2, \beta_2}(\omega_{\oplus})),$$

we verify the following properties:

- Positivity: $d_{\mathcal{G}}([\gamma_{\alpha_1, \beta_1}], [\gamma_{\alpha_2, \beta_2}]) \geq 0$, and $d_{\mathcal{G}}([\gamma_{\alpha_1, \beta_1}], [\gamma_{\alpha_2, \beta_2}]) = 0$ if and only if $\gamma_{\alpha_1, \beta_1} \sim \gamma_{\alpha_2, \beta_2}$.
- Symmetry: $d_{\mathcal{G}}([\gamma_{\alpha_1, \beta_1}], [\gamma_{\alpha_2, \beta_2}]) = d_{\mathcal{G}}([\gamma_{\alpha_2, \beta_2}], [\gamma_{\alpha_1, \beta_1}])$.
- Triangle inequality:

$$d_{\mathcal{G}}([\gamma_{\alpha_1, \beta_1}], [\gamma_{\alpha_2, \beta_2}]) \leq d_{\mathcal{G}}([\gamma_{\alpha_1, \beta_1}], [\gamma_{\alpha_3, \beta_3}]) + d_{\mathcal{G}}([\gamma_{\alpha_3, \beta_3}], [\gamma_{\alpha_2, \beta_2}]).$$

Positivity: By definition of the metric, $d_{\mathcal{G}}([\gamma_{\alpha_1, \beta_1}], [\gamma_{\alpha_2, \beta_2}]) \geq 0$. If $\gamma_{\alpha_1, \beta_1} \sim \gamma_{\alpha_2, \beta_2}$, then $\Gamma_{\alpha_1, \beta_1}(\omega) = \Gamma_{\alpha_2, \beta_2}(\omega)$ for all $\omega \in \mathcal{M}$, and thus:

$$d_{\mathcal{G}}([\gamma_{\alpha_1, \beta_1}], [\gamma_{\alpha_2, \beta_2}]) = d(\Gamma_{\alpha_1, \beta_1}(\omega_{\oplus}), \Gamma_{\alpha_2, \beta_2}(\omega_{\oplus})) = 0.$$

Conversely, if $d_{\mathcal{G}}([\gamma_{\alpha_1, \beta_1}], [\gamma_{\alpha_2, \beta_2}]) = 0$, then:

$$d(\Gamma_{\alpha_1, \beta_1}(\omega_{\oplus}), \Gamma_{\alpha_2, \beta_2}(\omega_{\oplus})) = 0,$$

which implies $\Gamma_{\alpha_1, \beta_1}(\omega) = \Gamma_{\alpha_2, \beta_2}(\omega)$ for all $\omega \in \mathcal{M}$, and therefore $\gamma_{\alpha_1, \beta_1} \sim \gamma_{\alpha_2, \beta_2}$.

Symmetry: By definition of the metric,

$$d_{\mathcal{G}}([\gamma_{\alpha_1, \beta_1}], [\gamma_{\alpha_2, \beta_2}]) = d(\Gamma_{\alpha_1, \beta_1}(\omega_{\oplus}), \Gamma_{\alpha_2, \beta_2}(\omega_{\oplus})).$$

Since the metric d on \mathcal{M} is symmetric, we have:

$$d(\Gamma_{\alpha_1, \beta_1}(\omega_{\oplus}), \Gamma_{\alpha_2, \beta_2}(\omega_{\oplus})) = d(\Gamma_{\alpha_2, \beta_2}(\omega_{\oplus}), \Gamma_{\alpha_1, \beta_1}(\omega_{\oplus})),$$

and thus:

$$d_{\mathcal{G}}([\gamma_{\alpha_1, \beta_1}], [\gamma_{\alpha_2, \beta_2}]) = d_{\mathcal{G}}([\gamma_{\alpha_2, \beta_2}], [\gamma_{\alpha_1, \beta_1}]).$$

Triangle inequality: Using the definition of the metric,

$$d_{\mathcal{G}}([\gamma_{\alpha_1, \beta_1}], [\gamma_{\alpha_2, \beta_2}]) = d(\Gamma_{\alpha_1, \beta_1}(\omega_{\oplus}), \Gamma_{\alpha_2, \beta_2}(\omega_{\oplus})).$$

By the triangle inequality for d on \mathcal{M} , we have:

$$d(\Gamma_{\alpha_1, \beta_1}(\omega_{\oplus}), \Gamma_{\alpha_2, \beta_2}(\omega_{\oplus})) \leq d(\Gamma_{\alpha_1, \beta_1}(\omega_{\oplus}), \Gamma_{\alpha_3, \beta_3}(\omega_{\oplus})) + d(\Gamma_{\alpha_3, \beta_3}(\omega_{\oplus}), \Gamma_{\alpha_2, \beta_2}(\omega_{\oplus})).$$

Substituting back into the metric on the quotient space, this becomes:

$$d_{\mathcal{G}}([\gamma_{\alpha_1, \beta_1}], [\gamma_{\alpha_2, \beta_2}]) \leq d_{\mathcal{G}}([\gamma_{\alpha_1, \beta_1}], [\gamma_{\alpha_3, \beta_3}]) + d_{\mathcal{G}}([\gamma_{\alpha_3, \beta_3}], [\gamma_{\alpha_2, \beta_2}]).$$

The quotient space $\mathcal{G}(\mathcal{M})/\sim$ with the metric

$$d_{\mathcal{G}}([\gamma_{\alpha_1, \beta_1}], [\gamma_{\alpha_2, \beta_2}]) = d(\Gamma_{\alpha_1, \beta_1}(\omega_{\oplus}), \Gamma_{\alpha_2, \beta_2}(\omega_{\oplus}))$$

satisfies positivity, symmetry, and triangle inequality, and is therefore a dometric space. \square

S.3.4 Proof of Theorem 4.1

Proof. By the definition of $d_{\mathcal{G}}$ and Assumption 4.2, we have

$$\begin{aligned} d_{\mathcal{G}}(\hat{\tau}, \tau) &= d_{\mathcal{G}}(\gamma_{\hat{\nu}'_{1,1}, \hat{\nu}_{1,1}}, \gamma_{\nu'_{1,1}, \nu_{1,1}}) \\ &= d(\Gamma_{\hat{\nu}'_{1,1}, \hat{\nu}_{1,1}}(\nu'_{1,1}), \Gamma_{\nu'_{1,1}, \nu_{1,1}}(\nu'_{1,1})) \\ &\leq C_2 \{d(\hat{\nu}'_{1,1}, \nu'_{1,1}) + d(\hat{\nu}_{1,1}, \nu_{1,1})\}. \end{aligned}$$

For the first term $d(\hat{\nu}'_{1,1}, \nu'_{1,1})$, applying the triangle inequality gives

$$\begin{aligned} d(\nu'_{1,1}, \hat{\nu}'_{1,1}) &= d(\Gamma_{\nu_{0,0}, \nu_{0,1}}(\nu_{1,0}), \Gamma_{\hat{\nu}_{0,0}, \hat{\nu}_{0,1}}(\hat{\nu}_{1,0})) \\ &\leq d(\Gamma_{\nu_{0,0}, \nu_{0,1}}(\nu_{1,0}), \Gamma_{\nu_{0,0}, \nu_{0,1}}(\hat{\nu}_{1,0})) + d(\Gamma_{\nu_{0,0}, \nu_{0,1}}(\hat{\nu}_{1,0}), \Gamma_{\hat{\nu}_{0,0}, \hat{\nu}_{0,1}}(\hat{\nu}_{1,0})). \end{aligned}$$

Using Assumptions 4.1 and 4.2, we further obtain

$$d(\nu'_{1,1}, \hat{\nu}'_{1,1}) \leq C_1 d(\hat{\nu}_{1,0}, \nu_{1,0}) + C_2 \{d(\hat{\nu}_{0,0}, \nu_{0,0}) + d(\nu_{0,1}, \hat{\nu}_{0,1})\}.$$

Combining these results, we have

$$d_{\mathcal{G}}(\hat{\tau}, \tau) \leq C_1 C_2 d(\hat{\nu}_{1,0}, \nu_{1,0}) + C_2^2 d(\hat{\nu}_{0,0}, \nu_{0,0}) + C_2^2 d(\nu_{0,1}, \hat{\nu}_{0,1}) + C_2 d(\hat{\nu}_{1,1}, \nu_{1,1}).$$

Under Assumption 4.3 and by [Petersen and Müller \(2019\)](#), Theorem 2, Assumptions A.1–A.3 imply that

$$d(\hat{\nu}_{d,t}, \nu_{d,t}) = O_p(n^{-1/(2(\kappa-1))}), \quad d, t \in \{0, 1\}.$$

Substituting these convergence rates into the above inequality, we conclude

$$d_{\mathcal{G}}(\hat{\tau}, \tau) = O_p(n^{-1/(2(\kappa-1))}).$$

□

S.3.5 Proof of Theorem 7.1

Proof. We first show (i). Observe that for $s = g - \delta - 1$,

$$\begin{aligned} \beta_{s+1} &= \Gamma_{E_{\oplus}(Y_{i,s}|C_i=1), E_{\oplus}(Y_{i,s+1}|C_i=1)}(\beta_s) \\ &= \Gamma_{E_{\oplus}(Y_{i,s}(0)|C_i=1), E_{\oplus}(Y_{i,s+1}(0)|C_i=1)}(E_{\oplus}(Y_{i,s}(0)|G_{i,g} = 1)) \\ &= E_{\oplus}(Y_{i,s+1}(0)|G_{i,g} = 1), \end{aligned}$$

where the second equality follows from Assumptions 7.1 and 7.2, and the third equality follows from Assumption 7.3. Likewise, we have $\beta_s = E_{\oplus}(Y_{i,s}(0)|G_{i,g} = 1)$, $s = \min\{g - \delta, t - 1\}, \dots, t$. Then we have

$$\begin{aligned} \gamma_{\beta_t, E_{\oplus}(Y_{i,t}|G_{i,g}=1)} &= \gamma_{E_{\oplus}(Y_{i,t}(0)|G_{i,g}=1), E_{\oplus}(Y_{i,t}|G_{i,g}=1)} \\ &= \gamma_{E_{\oplus}(Y_{i,t}(0)|G_{i,g}=1), E_{\oplus}(Y_{i,t}(g)|G_{i,g}=1)} \\ &= \tau(g, t), \end{aligned}$$

where the second equality follows from the definition of potential outcomes.

Next, we show (ii). Observe that for $s = g - \delta - 1$,

$$\begin{aligned}\beta_{s+1} &= \Gamma_{\nu_s, \nu_{s+1}}(\beta_s) \\ &= \Gamma_{\nu_s, \nu_{s+1}}(E_{\oplus}(Y_{i,s}(0)|G_{i,g} = 1)) \\ &= E_{\oplus}(Y_{i,s+1}(0)|G_{i,g} = 1),\end{aligned}$$

where the second equality follows from Assumptions 7.1 and 7.2, and the third equality follows from Assumption 7.4. Likewise, we have $\beta_s = E_{\oplus}(Y_{i,s}(0)|G_{i,g} = 1)$, $s = \min\{g - \delta, t - 1\}, \dots, t$. Then we have

$$\begin{aligned}\gamma_{\beta_t, E_{\oplus}(Y_{i,t}|G_{i,g}=1)} &= \gamma_{E_{\oplus}(Y_{i,t}(0)|G_{i,g}=1), E_{\oplus}(Y_{i,t}|G_{i,g}=1)} \\ &= \gamma_{E_{\oplus}(Y_{i,t}(0)|G_{i,g}=1), E_{\oplus}(Y_{i,t}(g)|G_{i,g}=1)} \\ &= \tau(g, t),\end{aligned}$$

where the second equality follows from the definition of potential outcomes. \square

S.3.6 Proof of Corollary 7.1

Proof. We only show (i) since (ii) can be shown almost in the same way. Observe that

$$\begin{aligned}E_{\oplus}[Y_{i,t}(0)|G_{i,g} = 1] &= \beta_t \\ &= \Gamma_{\alpha_{t-1}, \alpha_t}(\beta_{t-1}) \\ &\quad \vdots \\ &= (\Gamma_{\alpha_{t-1}, \alpha_t} \circ \dots \circ \Gamma_{\alpha_{g-\delta-1}, \alpha_{g-\delta}})(\beta_{g-\delta-1}) \\ &= \Gamma_{\alpha_{g-\delta-1}, \alpha_t}(\beta_{g-\delta-1}),\end{aligned}$$

where $\alpha_s = E_{\oplus}(Y_{i,s}(0)|C_i = 1)$, $s = g - \delta - 1, \dots, t$. Then we obtain

$$\begin{aligned}
& \ominus \gamma_{E_{\oplus}(Y_{i,g-\delta-1}|C_i=1), E_{\oplus}(Y_{i,t}|C_i=1)} \oplus \gamma_{E_{\oplus}(Y_{i,g-\delta-1}|G_{i,g}=1), E_{\oplus}(Y_{i,t}|G_{i,g}=1)} \\
& = \gamma_{\Gamma_{\alpha_{g-\delta-1}, \alpha_t}(\beta_{g-\delta-1}), E_{\oplus}(Y_{i,t}(g)|G_{i,g}=1)} \\
& = \gamma_{\beta_t, E_{\oplus}(Y_{i,t}(g)|G_{i,g}=1)} \\
& = \tau(g, t),
\end{aligned}$$

where the first equality follows from the definition of potential outcomes. □